

---

Satellite Products and Services Review Board

**Algorithm Theoretical  
Basis Document  
for NOAA NDE OMPS  
Version 8 Ozone Profile (V8PRO)  
Environmental Data Record (EDR)  
Version 1.0**



---

TITLE: FOR NOAA NDE OMPS VERSION 8 OZONE PROFILE

AUTHORS:

Lawrence Flynn NOAA STAR

Zhihua Zhang (IMSG)

Valerie Mikles (IMSG)

Bigyani Das (IMSG)

Jianguo Niu (SRG)

C. Trevor Beck (STAR)

Eric Beach (IMSG)

APPROVAL SIGNATURES:

---

Lihang Zhou (STAR)  
STAR JPSS Lead

Date

Remarks: This document shares algorithm descriptive material with the corresponding NASA-sponsored Version 8 Ozone Profile algorithm theoretical basis document.

**DOCUMENT HISTORY  
DOCUMENT REVISION LOG**

The Document Revision Log identifies the series of revisions to this document since the baseline release. Please refer to the above page for version number information.

<b>DOCUMENT TITLE: Algorithm Theoretical Basis Document Template</b>			
<b>DOCUMENT CHANGE HISTORY</b>			
<b>Revision No.</b>	<b>Date</b>	<b>Revision Originator Project Group</b>	<b>CCR Approval # and Date</b>
1.0	9/1/2016	L. Flynn	
1.1	3/10/2017	L. Flynn	



# TABLE OF CONTENTS

	<u>Page</u>
LIST OF TABLES AND FIGURES.....	8
1. INTRODUCTION.....	9
1.1. Product Overview.....	9
1.1.1. Product Description.....	9
1.1.2. Product History.....	9
1.1.3. Product Requirements.....	9
1.2. Satellite Instrument Description.....	10
2. ALGORITHM DESCRIPTION.....	11
2.1. Processing Outline.....	11
2.2. Algorithm Input.....	26
2.2.1. Input Satellite Data.....	26
2.2.2. Satellite Data Preprocessing Overview.....	26
2.2.3. Input satellite data description.....	26
2.2.4. Input Ancillary Data – Climatolgy and RT LUTs.....	27
2.3. Theoretical Description.....	28
2.3.1. Physical Description.....	28
2.3.2. Mathematical Description.....	31
Forward Model.....	31
Single Scattering Forward Model.....	32
Multiple Scattering Forward Model.....	33
Spectroscopic Constants.....	34
2.3.3. Retrieval Algorithm.....	34
2.3.4. Version 8 Algorithm A Priori Profiles.....	34
2.3.5 Retrieval Formulation.....	35
2.3.6. Averaging Kernels.....	36
2.3.7 Error Analysis.....	39
Forward Model Errors.....	40
Inverse Model Errors.....	40
Temperature.....	41
2.3.8. Instrumental Errors.....	41
Radiometric Calibration.....	43
Stray Light.....	44
Wavelength Scale and Bandpass.....	46
2.4. Algorithm Output.....	47
2.5. Performance Estimates.....	51
2.5.1. Test Data Description.....	51
2.5.2. Sensor Effects.....	51
2.5.3. Retrieval Errors.....	52
2.5.4. Numerical Computation Considerations.....	53
2.5.5. Programming and Procedural Considerations.....	54

2.5.6. Quality Assessment and Diagnostics.....	54
2.5.7. Exception Handling .....	54
2.6. Validation .....	54
3. ASSUMPTIONS AND LIMITATIONS.....	54
3.1. Performance Assumptions.....	54
3.2. Potential Improvements.....	55
4. REFERENCES .....	56

## LIST OF TABLES AND FIGURES

Table 2-1 OMPS SDR and GEO data used by the NDEV8P algorithm .....	26
Table 2-2 Satellite, Climatological and Table data used by the NDEV8P algorithm.....	27
Table 2-3 NDE Ozone Profile File.....	47
Table 2-4 Ozone Profile Output Granule File Content .....	47
Table 2-5 Ozone Profile Performance Requirements .....	52
Figure 2.1: The Flow Charts (Chart 1, Chart 2, Chart 3 and Chart 4) .....	24
Figure 2-3: Sample ozone weighting functions for the seven shortest SBUV/2 channels .....	30
Figure 2-4: A Sample of Solar Irradiance (Top), Earth radiance (Middle), and Earth albedo (Bottom) measured by NOAA-17 SBUV/2.....	32
Figure 2-5a: Averaging kernel as fractional layer changes for an equatorial profile and viewing condition.....	37
Figure 2-5b: Averaging kernel as fractional layer changes for a mid-latitude profile and viewing condition.....	38
Figure 2-5c: Averaging kernels as fractional layer changes for a high latitude profile and viewing condition.....	38
Figure 2-6: Difference in retrieval responses for $\pm 1\%$ uniform measurement errors at all profiling wavelengths at 16 latitudes (every $10^\circ$ from 75S to 75N).....	42
Figure 2-7: Difference in retrieval response for $-0.5\%$ measurement errors at individual profile wavelengths – 273, 283, 288, 292, 298 and 302-nm channels for the 273-nm to 302-nm channels at 45N latitude.....	43
Figure 2-8: Out-of-Band Stray Light for NOAA-17 SBUV/2 observed in Ground Test.....	44
Figure 2-9: Onset of In-band Stray Light at $77^\circ$ SZA as Seen in NOAA-17 .....	45
Figure 2-10: Signal Levels across a Hg-Lamp Line from Continuous Scan .....	46

## 1. INTRODUCTION

This document presents the scientific background, design and performance of the Ozone Mapping and Profiler Suite Nadir Profiler (OMPS NP) Version 8 Ozone Profile (V8PRO) Environmental Data Record (EDR) algorithm for the Joint Polar Satellite System (JPSS). The V8PRO algorithm produces a bundled set of outputs from OMPS NP and OMPS Nadir Mapper (NM) measurements.

Products from the OMPS V8PRO algorithm described here fulfill the requirements identified in the JPSS OMPS Ozone Profile. Furthermore, those requirements provide continuity to the NASA EOS Aura Ozone Monitoring Instrument (OMI).

### 1.1. Product Overview

#### 1.1.1. Product Description

Product description with sufficient detail so that the user understands how to use the product files. (*Document Object 34*)<sup>1</sup>

**Writers:** Algorithm Scientists.

The NDEV8P product was developed to generate Ozone Profile estimates from a discrete set of 13 measurements of backscattered ultraviolet radiances in the 250 nm to 380 nm range. It creates a 21-layer ozone retrieval along with measurement residuals, error flags and other retrieval parameters. In addition to the ozone profile retrieval, it also makes total ozone estimates, and produces effective UV reflectivity, absorbing aerosol index values and retrieval information such as measurement sensitivities and residuals and retrieval efficiency factors. The algorithm processes all daytime OMPS Nadir Profiler Sensor Data Records (SDRs). Details on the content of the NDEV8P external output files are provided in section 1.3.

#### 1.1.2. Product History

The NDEV8P is a new implementation of the Version 8 Ozone Profile retrieval algorithm developed by NASA GSFC for the Solar Backscatter Ultraviolet (SBUV(/2)) series of instruments and refined for use with the NASA EOS Aura Ozone Monitoring Instrument (OMI). NOAA has previously implemented this algorithm operationally to create products from measurements made by the NOAA POES SBUV/2 instruments.

This product replaces the current operational IDPS Ozone Profile IP and planned EDR products (IMOPO, OONPO and INPAK). The IDPS and NDE products meet the JPSS Level 1 requirements. The NDE product will also be consistent with the existing NOAA SBUV/2 records.

#### 1.1.3. Product Requirements

State the requirements for each product, either explicitly or by reference to the project's requirements document, if available. Product requirements should include content, format, latency, quality. (*Document Object 1*)

**Writers:** Development Lead.

All NDEV8P basic and derived requirements are available in the V8PRO Requirements Allocation Document (RAD). These requirements identify the users and their needs with respect to file content, format, latency, and quality. They are based on the Level 1 Requirements for Ozone Profile EDRs from the JPSS program.

## 1.2. Satellite Instrument Description

Describe the attributes of the sensing system(s) used to supply data for the retrieval algorithm at a level of detail sufficient for reviewers to verify that the instrument is capable of supplying input data of sufficient quality. (*Document Object 28*)

**Writers:** Development Lead and PAL should collaborate.  
(*Document Object 28*)

NDEV8P is a system operated within the NDE DHS by OSPO. It uses measurements from the Ozone Mapping and Profiler Suite (OMPS) Nadir Profiler (NP) and Nadir Mapper (NM) on the Suomi National Polar-orbiting Partnership (S-NPP) platform and will continue with OMPS on future satellites of the Joint Polar Satellite System (JPSS). S-NPP was launched on October 28, 2011. It is in a sun synchronous orbit with a 1:30 PM ascending-node orbit at an altitude of 829 km.

The OMPS NM instrument is a pushbroom spectrometer with a 2-dimensional CCD array detector. The telescope images a  $105^\circ$  cross-track FOV onto the array, providing full daily coverage of the sunlit Earth. It has 196 spectral bands covering the spectrum between 300 nm to 380 nm with 1.1 nm FWHM and 0.42-nm sampling. The instrument is highly flexible and is currently operated to aggregate approximately 20 spatial pixels into 35 cross-track bin and to integrate for approximately 7.8 S. This produces  $50 \times 50 \text{ km}^2$  size products at nadir. Plans for J-01 are to reduce both dimensions by a factor of three and create 103 cross track bins every 2.6 S with  $17 \times 17 \text{ km}^2$  size products at nadir.

The grating spectrometer and focal plane for total column measurements provide 0.42 nm spectral sampling across the wavelength range of 300 to 380 nm. The radiance/irradiance ratios for the four longer wavelengths used in the V8Pro EDR algorithm are obtained by interpolating the values at adjacent measurement wavelengths to provide them at the following wavelengths: [313, 318, 331.3, 360.2] nm.

The OMPS NP instrument is a nadir-viewing double monochromator with 2-dimensional CCD array detector. The same telescope provides the signal but only the central nadir  $14^\circ$  FOV is imaged on the detector. A dichroic element with a transition interval from 300 nm to 310 nm is used to split the signal into the NM and NP components. The NP has 147 bands with 0.42 nm spacing and 1.1 nm FWHM bandpasses from 250 nm to 310 nm. The radiance/irradiance ratios for the eight shorter wavelengths used in the V8Pro EDR algorithm are obtained by interpolating the values at adjacent measurement wavelengths to provide them at the following wavelengths: [253, 273, 283, 288, 292, 298, 302, 306] nm.

## 2. ALGORITHM DESCRIPTION

Radiation at the near-UV wavelengths is absorbed by ozone, such that the difference between the incoming and outgoing radiation can be related to the amount of ozone in the atmosphere. Radiation amounts at the eight shortest wavelength channels used in the V8PRO are absorbed by atmospheric ozone before reaching the surface, implying that radiation scattered back to the instrument came from a particular altitude range. Radiation at successively longer wavelengths penetrates deeper into the atmosphere before being completely absorbed by ozone, allowing for a measure of the ozone profile. In the Version 8 algorithm, the total ozone is also calculated as the sum of the retrieved profile ozone, rather than just from measurements at the four longest wavelengths, which do penetrate to the surface. This makes the total ozone less sensitive to the variations in surface reflectivity and scattering processes in the troposphere.

The NDEV8P product is generated from the Version 8 Ozone Profile algorithm (V8PRO). The V8PRO uses a new set of profiles for the *a priori* information leading to better estimates in the troposphere (where BUV measurements lack retrieval information) and to simplified comparisons of SBUV/2 and OMPS results to other measurement systems (in particular, the Umkehr ground-based O<sub>3</sub> profile retrievals which now use the same set of *a prioris*). The V8PRO has improved total O<sub>3</sub> retrievals from improved multiple scattering and cloud and reflectivity modeling. Some errors present in the V6A version will be reduced. These include a correction for 2% errors from previously ignoring the gravity gradient with height and elimination of 0.5% errors from low fidelity bandpass modeling. The V8PRO is also designed to allow the use of more accurate external and climatological data, to adjust for changes in wavelength selection, and to incorporate several *ad hoc* Version 6 algorithm improvements directly. Some components of the initial V8PRO implementation were optimized for trend detection. These are modified for use in operations but the algorithm has the flexibility to make these changes.

### 2.1. Processing Outline

Full description of the processing outline of the retrieval algorithm. All key elements and sub-elements needed to convey a comprehensive sense of the algorithm should be included. The level of detail should be consistent with the current maturity of the software architecture (which will improve with each revision). A data flow diagram consistent with the software architecture is preferred. (*Document Object 13*)

**Writers:** Algorithm Scientists.

The OMPS V8PRO is a self-contained algorithm with no dependencies on other Level 2 products. It reads input OMPS Sensor Data Record (SDR) and Geolocation Data Records (GEO) from both the NM and NP sensors and combines these with climatological and radiative transfer lookup table (RTLUT) input to generate the Ozone profile estimates. All OMPS Earth View SDRs on the dayside of the orbit are processed individually.

### Description modules of NDE-V8PRO algorithm:

Main program: O3P\_main.f90

Here is the description of all the routines used in this package.

**Subroutine altitude (altitude.f90)**

Subroutine altitude is a subroutine to compute the geophysical altitude based on temperature and pressure. It calculates physical heights at specified pressure levels.

Called by o3\_retrieval and profile.

**Subroutine aprsbo (stndprof.f90)**

Subroutine to read in a priori ozone.

Called by total.

**Subroutine aprsbt (stndprof.f90)**

Subroutine to read in a priori temperature.

Called by total.

**Subroutine blwclld (blwclld.f90)**

Subroutine blwclld is a subroutine to estimate the amount of ozone below a cloud pressure level using standard ozone profile climatology.

Called by total.

**Subroutine cnstnts (start.f90)**

Subroutine for initializing various constant parameters used in the retrieval.

Called by start.

Calls coffs.

**coffs (start.f90)**

Subroutine for assigning optical coefficients and weights for SBUV sub-channels.

Called by cnstnts.

**Module constants (constants.f90)**

Module constants is a model that sets parameters for total ozone retrievals.

**Module control (control.f90)**

Module control is a module that has indexing parameters to set which measurement values to use from the input nvalue.

**Subroutine copy\_geoloc\_to\_output (geo\_mod.f90)**

Subroutine copy\_geoloc\_to\_output is a subroutine to place geolocation data into the output.

Called by scanin.

**Subroutine convert20 (profile\_datamod.f90)**

Subroutine convert20 is a subroutine to convert 80 layer profiles to 20 layer ones.

Called by profile.

**Subroutine data\_ingest (data\_ingest.f90)**

Subroutine data\_ingest is a subroutine to prepare and ingest all necessary data to process version 8 ozone profile retrieval algorithm.

Calls `init_netcdf`, `fillval_retrieval_fields`, `total`, `profile`, `write_global_output`, `total_to_netcdf`, `profile_to_netcdf`.  
Called by `O3_main`.

### **Subroutine `dn_by_dt` (`dndt.f90`)**

Subroutines for computing the change in N-value due to temperature difference for each of 11 Umkehr layers and each of 8 wavelengths using a chain rule relating  $dN/dT$  to  $dN/dX$ . Subroutine `dndt` is a module to handle calculation of the temperature correction at the standard pressure layers.  
Called by `total` and `msr_temp_adjust`.

### **Subroutine `factor` (`linsolve.f90`)**

Subroutine `factor` is a subroutine for performing an LU factorization of a general matrix of dimension  $N \times N$ .  
Called by `update` and `convert20`.

### **Subroutine `fillval_retrieval_fields` (`output.f90`)**

Subroutine `fillval_retrieval_fields` is a subroutine for setting retrieved quantities to zero, initial values.  
Called by `data_ingest`.

### **Module `geo_mod` (`geo_mod.f90`)**

Module `geo_mod` is a Module to track the geolocation and viewing geometry of the observation. Module to store ground pixel level information such as snow ice, cloud pressure, and measurement geometry.

### **Subroutine `getmsr` (`getmsr.f90`)**

Subroutine `getmsr` is a subroutine to compute nvalues from radiative transfer tables specific to the version 8 total ozone channel. It computes the multiple scattered and surface reflected part of the Jacobian for each of 11 Umkehr layers and each of 8 wavelengths by using finite differencing between N-values interpolated from unperturbed and perturbed ozone tables. 12 tables are contained in common: 1 unperturbed followed by 11 with perturbations in Umkehr layers 0–9 and the sum of layers 10-12.  
Calls `getmsr_single_chan`.  
Called by `total`.

### **Function `getfilename` (`O3P_input_class.f90`)**

Function `getfilename` is for reading in file names from control file.  
Called by `O3P_main`.

### **Subroutine `getrng` (`getrng.f90`)**

Subroutine `getrng` is a subroutine for interpolating appropriate ring effect corrections in reflectivity and pressure. This is the RRS (Rotational Raman Scattering) correction. This corrects for inelastic scattering in the atmosphere from molecular oxygen and nitrogen.  
Called by `reflec` and `residue`.

### **Subroutine `getshape` (`getshape.f90`)**

Subroutine getshape is a subroutine to compute an ozone a priori profile from climatology based on total ozone, day of year and latitude.  
Called by total.

**Subroutine init\_dndt (dndt.f90)**

Subroutine init\_dndt.f90 is a subroutine to initialize ozone absorption coefficients for profile channels.  
Called by start.

**Subroutine init\_dndt\_toz (dndt.f90)**

Subroutine init\_dndt\_toz is a subroutine to initialize ozone absorption coefficients for total ozone channels.  
Called by start.

**Subroutine init\_netcdf (netcdf\_util.f90)**

Subroutine init\_netcdf is a subroutine to declare dimensions and variables for writing out data in NetCDF format.  
Called by data\_ingest.

**Subroutine init\_retrieval (init\_retrieval.f90)**

Subroutine init\_retrieval.f90 is a subroutine that performs initial input of v8pro required ancillary data.  
Calls start.  
Called by O3P\_main.

**Subroutine inter (inter.f90)**

Subroutine inter is a module to interpolate climatological values of snow ice, surface type, and cloud pressure. The subroutine within it are run to find terrain, cloud pressure, snow/ice, and surface category code from appropriate data bases for a given date, latitude and longitude.  
Called by scanin.  
Calls insurf and incovr.

**Subroutine interp\_dndx (msr.f90)**

Subroutine interp\_dndx is a subroutine to interpolate table entries.  
Called by getmsr\_single\_chan and msr\_component.

**Subroutine interp\_rad (msr.f90)**

Subroutine interp\_rad is a subroutine to interpolate table entries in pressure.  
Called by rad\_msr and iztrsb.  
Calls interp\_sza\_vza.

**Subroutine interp\_sza\_vza (msr.f90)**

Subroutine interp\_sza\_vza is a subroutine to interpolate table entries in solar and viewing angles.  
Called by interp\_rad.

**Subroutine interpol\_kern (interpol\_kern.f90)**

Subroutine interpol\_kern is a subroutine to interpolate a multiple scattering kernel to a finer pressure level.

Called by profile.

**Subroutine interpol\_qo3 (interpol\_qo3.f90)**

Subroutine interpol\_qo3 is a subroutine to convert a 21-layer ozone profile into 81 layers on a finer pressure grid.

Calls splinev8.

Called by profile.

**Subroutine interpol\_t (interpol\_t.f90)**

Subroutine interpol\_t uses splines to convert a 21-layer climatological temperature profile to the 81-layer temperature profile used in the ozone profile retrieval.

Calls splinev8.

Called by profile.

**Subroutine inverse (linsolve.f90)**

Subroutine inverse inverts a matrix.

Called by o3\_retrieval, convert20, and update.

**Subroutine iztrsb (iztrsb.f90)**

Subroutine iztrsb is a subroutine to compute components of the nvalue calculation from radiative transfer tables. It performs interpolations of the table parameters  $i0$ ,  $rT$ , and  $Sb$ , which are used by the calling routines to calculate table radiances or N-values. It uses Lagrangian interpolation except for high clouds for which a linear extrapolation is used.

Called by oznot, refl\_360, reflc, and residue.

Calls interp\_rad.

**Subroutine linear\_fit (linear\_fit.f90)**

Subroutine linear\_fit is a subroutine to do a linear least squares fit of a set of points.

Called by o3\_retrieval.

**Module lpoly (lpoly.f90)**

Module lpoly is a module to define lagrangian interpolation coefficients. Used in interp\_dndx, interp\_sza\_vza, scanin, and cnstnts.

**Subroutine mixratio (mixratio.f90)**

Subroutine mixratio is a subroutine to compute the volume mixing ratio estimated ozone profile using the current estimated ozone in DU (Dobson Unit). It determines ozone mixing ratio and its estimated percentage error at prescribed pressure levels.

Called by profile.

Calls splinev8.

**Module msr (msr.f90)**

Module msr is a module that has subroutines to compute nvalues from radiative transfer tables.

**Module msr\_temp\_adjust (msr.f90)**

Subroutine `msr_temp_adjust` is a subroutine to compute adjustments for temperature differences.

Calls `dn_by_dt`.

Called by `total`.

#### **Subroutine `nvbrac` (`oznot.f90`)**

Subroutine `nvbrac.f90` is a subroutine to perform N-value bracketing and prepare for interpolation.

Called by `oznot`.

#### **Subroutine `o3_retrieval` (`o3_retrieval.f90`)**

Subroutine `o3_retrieval` is a subroutine to carry out the version 8 ozone retrieval using maximum likelihood estimation. It performs ozone retrievals by using Rodgers method.

Calls `linear_fit`, `altitude`, `o3_snglscatt`, `update` and `inverse`.

Called by `profile`.

#### **Subroutine `o3_snglscatt` (`o3_snglscatt.f90`)**

Subroutine `o3_snglscatt` is a subroutine that is the primary single scatter radiative transfer calculator. It computes the ozone single scattering approximation.

Called by `o3_retrieval`.

#### **module `O3P_input_class` (`O3P_input_class.f90`)**

Module `O3P_input_class` Contains the functions that read in the namelist from control file (`getFileName`) and read in geo/sdr data from IDPS outputs , and makes module `O3T_input_class.mod`.

Calls `getfilename`, `rd_gotco`, `rd_somtc`, `rd_somps` and `rd_gonpo`.

Called by `O3P_main`.

#### **program `O3P_main` (`O3P_main.f90`)**

Program `O3P_main` is the main program that reads in control file, which contains all input, file (SDR and ancillary data) needed for processing `v8profile` algorithm. The program performs searching and averaging TC data within NP FOV, and makes interpolation of earth radiance and solar flux into target wavelengths that used in the `V8PRO` retrieval. The program also acts as an interface to the `v8profile` retrieval code.

Calls `init_retrieval`, `data_indest`.

#### **Subroutine `oznot` (`oznot.f90`)**

Subroutine `oznot` is a subroutine to compute initial ozone estimate using the 317.5 nm channel.

Called by `total`.

Calls `iztrsb`, `getrngand` and `nvbrac`.

#### **Subroutine `ozone` (`ozone.f90`)**

Subroutine `ozone` is a subroutine to compute `step3` ozone or best ozone for the total ozone algorithm.

Called by `total`.

#### **Module `output` (`output.f90`)**

Module output is a module that stores values for output.

**Function pintrp (pterp.f90)**

Function pintrp is a function to set up pressures for interpolation.

**Subroutine prfind (reflec.f90)**

Subroutine prfind finds table entries for reflectivity computations.  
Called by reflec.

**Module pterp (pterp.f90)**

Module pterp is a module to interpolate in pressure using lagrangian interpolation method.

**Module press\_interp (msr.f90)**

Function press\_interp is a function to interpolate in pressure using lagrangian interpolation.  
Called in interp\_rad.

**Subroutine profile (profile.f90)**

Subroutine profile is a high-level subroutine that does the ozone profile estimation. This is the subdriver for profile ozone retrieval.

Calls Interpol\_qo3, Interpol\_t, Interpol\_kern, o3\_retrieval, set\_profile\_output, convert20, mixratio, altitude, and splinev8.

Called by data\_ingest.

**Module profile\_data\_module (profile\_datamod.f90)**

Module profile\_data\_module is a module that stores input data to the ozone profile estimation algorithm.

**Subroutine profile\_to\_netcdf (netcdf\_util.f90)**

Subroutine profile\_to\_netcdf is a subroutine to write profile ozone calculation results for NetCDF formatted output file.

Called by data\_ingest.

**Subroutine rad\_msr (msr.f90)**

Subroutine rad\_msr is a subroutine to perform N-value table computations.

Calls interp\_rad.

Called by total.

**Subroutine rdcons (constants.f90)**

Subroutine rdcons is in constants.f90. It is a subroutine that stores constants used in the Version 8 retrieval. It reads in instrument dependent constants.

Called by start.

Calls set\_best\_ozone\_chans.

**Subroutine RD\_GOTCO (O3P\_input\_class.f90)**

Subroutine RD\_GOTCO is a subroutine that reads in HDF formatted NM GEO file.

Called by O3\_main.

**Subroutine RD\_GONPO (O3P\_input\_class.f90)**

Subroutine RD\_GONPO is a subroutine that reads in HDF formatted NP GEO file.  
Called by O3\_main.

**Subroutine RD\_SOMTC (O3P\_input\_class.f90)**

Subroutine RD\_SOMTC is a subroutine that reads in HDF formatted NM SDR file.  
Called by O3\_main.

**Subroutine RD\_SOMPS (O3P\_input\_class.f90)**

Subroutine RD\_SOMPS is a subroutine that reads in HDF formatted NP SDR file.  
Called by O3\_main.

**Subroutine read\_clim (stndprof.f90)**

Subroutine read\_clim is a subroutine to read in climatological profiles.  
Called by start.

**Subroutine read\_instrument\_table (msr.f90)**

Subroutine read\_instrument table is a subroutine to read in instrument tables.  
Called by read\_msr\_tables.

**Subroutine read\_instrument\_dndx (msr.f90)**

Subroutine read\_instrument\_dndx is a subroutine to read in instrument sensitivity tables.  
Called by read\_msr\_tables.

**Subroutine read\_msr\_tables (msr.f90)**

Subroutine read\_msr\_tables is a subroutine to read in multiple scattering tables.  
Called by start.  
Calls read\_instrument\_table and read\_instrument\_dndx.

**Subroutine reflec (reflec.f90)**

Subroutine reflec is a subroutine to compute reflectivity values using measured nvalue and computed nvalue.  
Calls pfind, iztrsb and getrng.  
Called by total.

**Subroutine refl\_360 (refl\_360.f90)**

Subroutine refl\_360 is a subroutine to compute the reflectivity at the longest wavelength measurement.  
Calls iztrsb.  
Called by total.

**Subroutine resadj (resadj.f90)**

Subroutine resadj is a subroutine that adjusts total ozone residual values from dndx values after calculation of best ozone.  
Called by total.

**Subroutine residue (residue.f90)**

Subroutine residue is a subroutine to compute the difference between a computed nvalue and measured nvalue. It computes the residues for each of the multiple scattered wavelengths.

Calls residue\_single\_chan.  
Called by total.

**Subroutine residue\_single\_chan (residue.f90)**

Subroutine residue\_single\_chan is a subroutine to compute residuals for single channels.  
Calls iztrsb and getrng.  
Called by residue.

**Subroutine scanin (scanin.f90)**

Subroutine scanin is a counterpart to the v6 scanin subroutine. It sets internal parameters based on solar zenith angle and surface pressure.  
Calls inter and copy\_geoloc\_to\_output.  
Called by total.

**Subroutine set\_best\_ozone\_chans (control.f90)**

Subroutine to set the ozone channels.  
Called by rdcons.

**Subroutine seterr (seterr.f90)**

Subroutine seterr is a subroutine to set error flags for the version 8 total ozone algorithm.  
Subroutine for setting error flags.  
Called by total.

**Subroutine set\_profile\_output (profile.f90)**

Subroutine set\_profile\_output is a subroutine to load profile ozone variables for a scan.  
Calls altitude and splinev8.  
Called by profile.

**Subroutine set\_total (total.f90)**

Subroutine set\_total is a subroutine to load total ozone variables for a scan.  
Called by total.

**Subroutine splinev8 (splinev8.f90)**

Subroutine splinev8 is a subroutine to perform clamped cubic spline implementation.  
Called by interpol\_qo3, interpol\_t, mixratio, and profile.

**Subroutine start (start.f90)**

Subroutine start is a subroutine to initialize startup values for the version 8 retrieval.  
Calls read\_clim, rdcons, cnstnts, read\_msr\_tables, init\_dndt, and init\_dndt\_toz.  
Called by init\_retrieval.

**Module stndprof (stndprof.f90)**

Module stndprof is a module that provides subroutines (aprsbo, aprsbt, and read\_clim) to interpolate standard ozone profiles to determine a priori ozone profile for a given day and latitude.

**Subroutine stnp81 (stnp81.f90)**

Subroutine stnp81 is a subroutine to determine a standard profile associated with a specific total ozone value and a single latitude band.  
Called by total.

**Subroutine total (total.f90)**

Subroutine total is a subroutine that carries out the high-level management of the total ozone retrieval. It is the driver for processing one scan of data from the level 1 SBUV record and computing the total ozone used as first guess in the profiling algorithm.  
Calls scaninv8, reflcv8, refl\_360, oznot, residue, rad\_msr, getmsr, msr\_component, aprsbo, aprsbt, stnp81, dn\_by\_dt, resadj, msr\_temp\_adjust, getshape, ozone, resadj, blwcl, seterr and set\_total\_output.  
Called by data\_ingest.

**Subroutine total\_to\_netcdf (netcdf\_util.f90)**

Subroutine total\_to\_netcdf is a subroutine to write total ozone calculation results for NetCDF formatted output file.  
Called by data\_ingest.

**Module totret (totret.f90)**

Module totret is a module to store data values for the v8pro total ozone algorithm.

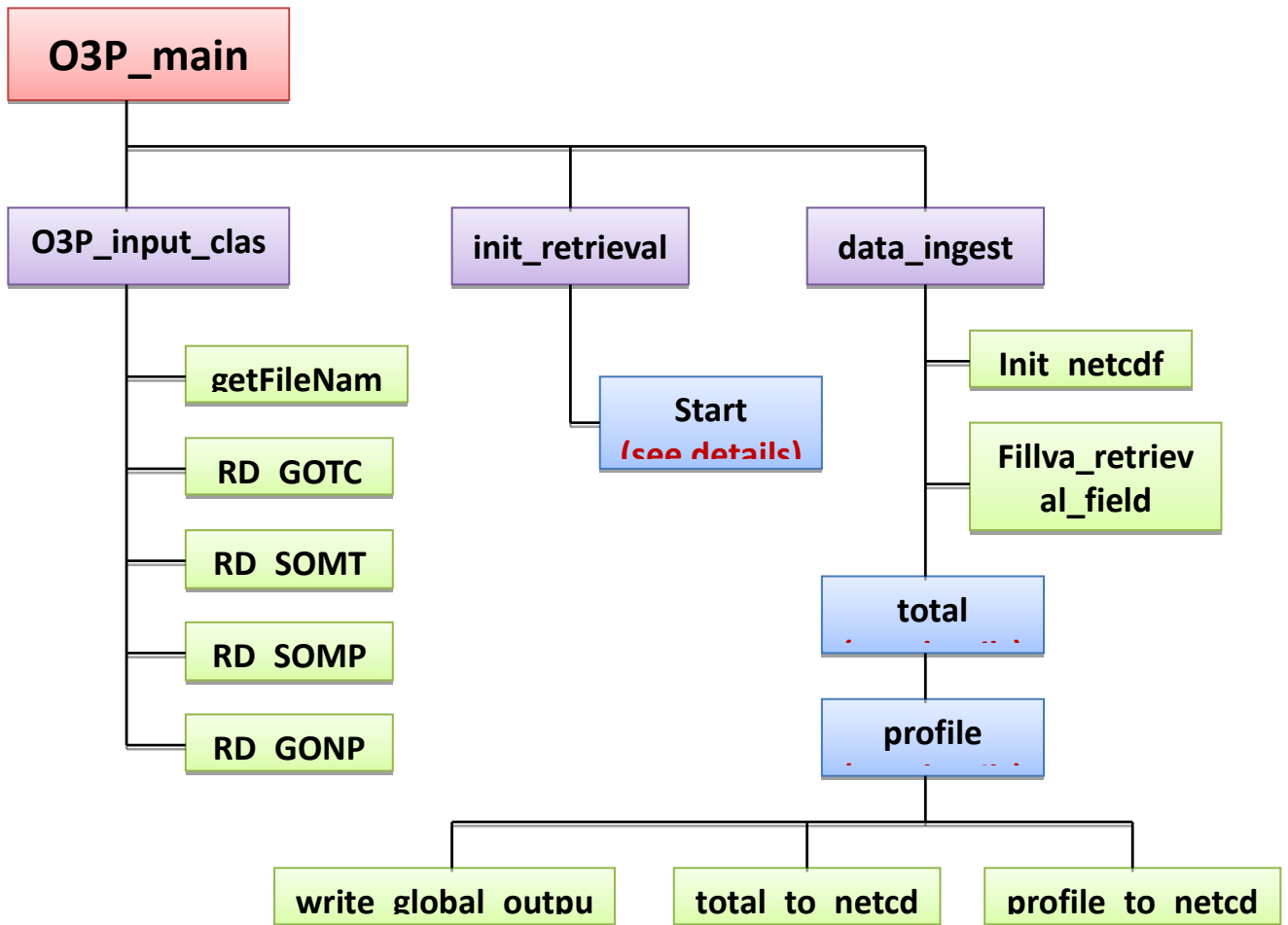
**Subroutine update (update.f90)**

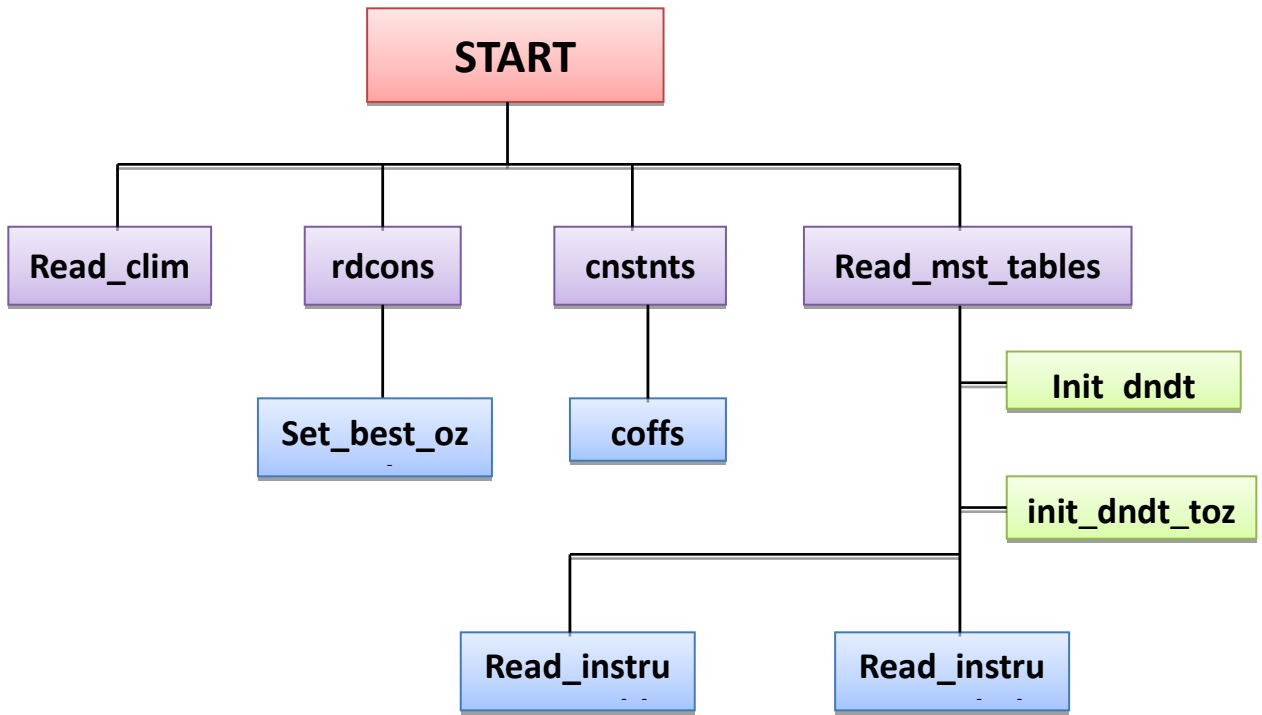
Subroutine update is a subroutine to carry out maximum likelihood estimation computations. It updates the ozone profile using C. Rodgers' method. Calls factor and inverse.  
Called by o3\_retrieval.

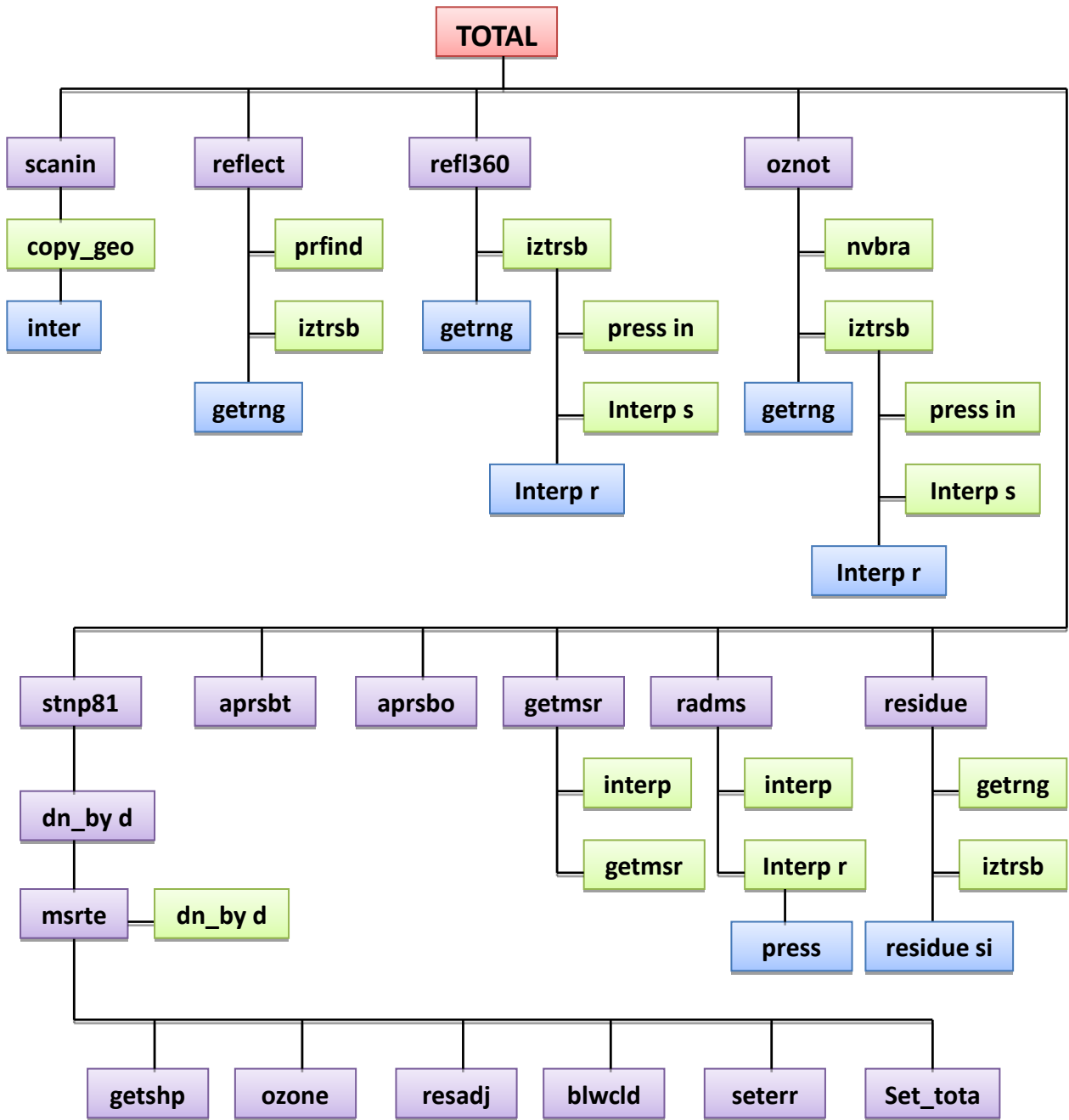
**Subroutine write\_global\_output (netcdf\_util.f90)**

Subroutine write\_global\_output is a subroutine to write global variables and attributes for NetCDF formatted output file.  
Called by data\_ingest.

**FLOW CHARTS FOR V8PRO**







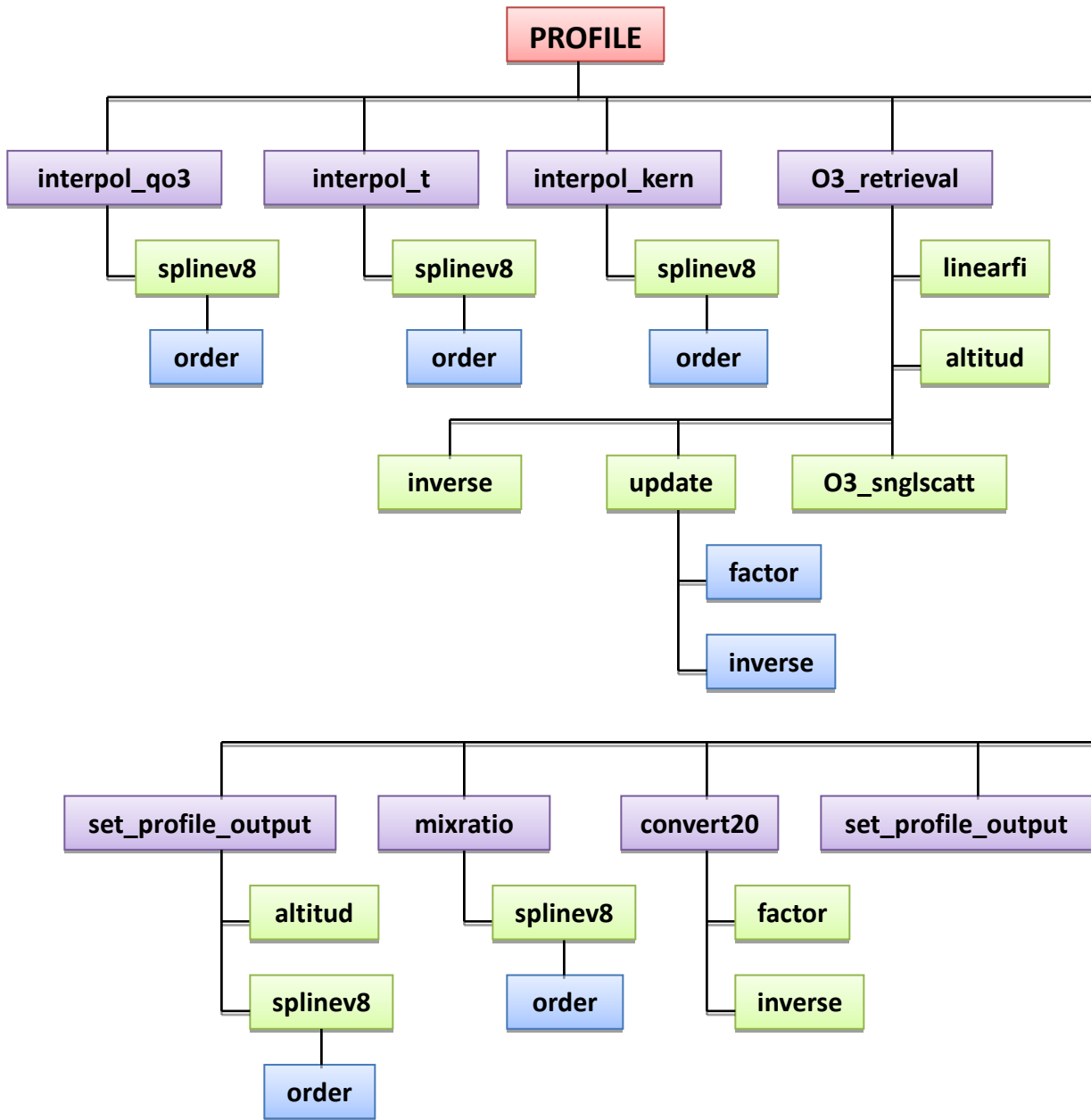


Figure 2.1: The Flow Charts (Chart 1, Chart 2, Chart 3 and Chart 4)

### The modules for NDE-V8PRO algorithm:

The OMPS NP V8 main source code consists of 13,108 lines in 45 files. It is written in FORTRAN 90 language.

The routines are:

- altitud.f90
- blwcd.f90
- constants.f90

control.f90  
data\_ingest.f90  
dndt.f90  
geo\_mod.f90  
getmsr.f90  
getrng.f90  
getshape.f90  
init\_retrieval.f90  
inter.f90  
interpol\_kern.f90  
interpol\_qo3.f90  
interpol\_t.f90  
iztrsb.f90  
linear\_fit.f90  
linsolve.f90  
lpoly.f90  
mixratio.f90  
msr.f90  
netcdf\_util.f90  
O3P\_input\_class.f90  
O3P\_main.f90  
o3\_retrieval.f90  
o3\_snglscatt.f90  
output.f90  
oznot.f90  
ozone.f90  
profile\_datamod.f90  
profile.f90  
pterp.f90  
refl\_360.f90  
reflec.f90  
resadj.f90  
residue.f90  
scanin.f90  
seterr.f90  
splinev8.f90  
start.f90  
stndprof.f90  
stnp81.f90  
total.f90  
totret.f90  
update.f90

## 2.2. Algorithm Input

Full description of the attributes of all input data used by the algorithm, including primary sensor data, ancillary data, forward models (e.g. radiative transfer models, optical models, or other model that relates sensor observables to geophysical phenomena) and look-up tables. Do not include file formats; these will be documented elsewhere. (*Document Object 14*)

**Writers:** Algorithm Scientists.

### 2.2.1. Input Satellite Data

#### 2.2.2. Satellite Data Preprocessing Overview

The OMPS Raw Data Records (RDRs) are processed at IDPS into Sensor Data Records (SDRs) by the OMPS NP SDR and OMPS NP geolocation algorithms. This processing includes the geolocation and radiometric calibration of the raw sensor output. Details of the OMPS SDR algorithm are described in the JPSS OMPS SDR ATBD. OMPS NP EDR algorithm also requires OMPS NM SDR and geolocation data.

#### 2.2.3. Input satellite data description

The NDEV8P algorithm uses the radiance and irradiance measurements provided in the OMPS NP and NM SDR and the geolocation and viewing geometry information provided in the OMPS NP and NM GEO. Table 2-1 provides a summary of the OMPS SDR and GEO parameters used by the algorithm.

**Table 2-1 OMPS SDR and GEO data used by the NDEV8P algorithm**

Input	Type	Description	Units/Valid Range
Pixel-Level Data Items			
satza	real	Satellite zenith angle	Degrees
sza	real	Solar zenith angle	Degrees
xphi	real	Relative azimuth angle between sensor and solar azimuth angles	Degrees
month	integer	Month of measurement	Month / 1 – 12
day	integer	Day of month of measurement	Day
seconds	long interger	Seconds in day of measurement	Seconds
xlat	real	Latitude of measurement	Degrees / -90 – 90
xlong	real	Longitude of measurement	Degrees / -180 – 180
xm	real	Radiances for 26 sensor wavelengths	W/m <sup>2</sup> -nm / 0 – 3x10 <sup>7</sup>
Sflux	real	Solar flux for 26 sensor wavelengths	W/m <sup>2</sup> -nm / 0 – 3x10 <sup>7</sup>

#### 2.2.4. Input Ancillary Data – Climatology and RT LUTs

The NDEV8P uses climatological values for Cloud Top Pressure, Snow/Ice Fields, and Surface Pressure and for Ozone and Temperature Profiles. It also uses radiative transfer Look-Up Tables to provide estimates of the top-of-atmosphere radiance/irradiance ratios (and their sensitivities to ozone layer perturbations) for standard ozone profiles and a select array of viewing conditions. Table 2-2 provides a summary of the climatological and table parameters used by the algorithm.

**Table 2-2 Satellite, Climatological and Table data used by the NDEV8P algorithm**

File Type	No.	Filename	Content	Data Format
Control File	1	namelist.nml	Runtime parameters (generated by driver script)	ASCII
IDPS Granule File	2	SOMPS_npp_IDP STime <sup>s</sup> _noaa_ops.h5	IDPS outputs of SDR data	HDF5
	3	GONPO_npp_IDP STime <sup>s</sup> _noaa_ops.h5	IDPS outputs of GEO data	HDF5
	4	SOMTC_npp_IDP STime <sup>s</sup> _noaa_ops.h5	IDPS outputs of SDR data for OMPS NM	HDF5
	5	GOTCO_npp_IDP STime <sup>s</sup> _noaa_ops.h5	IDPS outputs of GEO data for OMPS NM	HDF5
Ancillary File	6	band_centers.txt	Wavelengths and assumed bandpass FWHM for each measurement channel	ASCII
	7	cloud_ground_pressure.nc	Cloud pressure data	netCDF
	8	mrgapprf.dat	Merged a priori ozone climatology	ASCII
	9	O3_CLIM13.DAT	A priori ozone profile climatology	ASCII
	10	profile_dndx.nc	Profile N-value sensitivity look-up table	netCDF

	11	profile_table.nc	Profile N-value look-up table	netCDF
	12	solar_bass.dat	Solar radiation reference look-up table	ASCII
	13	TM_CLIM13.DAT	A priori temperature profile climatology	ASCII
	14	v8std81.dat	Standard profiles in fine layers	ASCII

<sup>s</sup>IDPSTime=dyyyyymmdd\_thhmmss0\_ehhmmss0\_b21447\_cyyyyymmddhhmmssxxxxxx, where the first character d, t, e, b, c, indicate the date, starting time, ending time, orbital number, creation time, and yyyy, mn, dd indicate the year, month, and day, while hh and the second mm, indicate the hour, minute. The ss0 and sxxxxx give tenths of seconds and microseconds respectively.

## 2.3. Theoretical Description

### 2.3.1. Physical Description

Comprehensively describe the sensor physics and the associated geophysical phenomenology key to the product retrieval. (*Document Object 15*)

**Writers:** Algorithm Scientists.

The Version 8 O3 profile algorithm (V8PRO) is the latest in a series of BUV (backscattered ultraviolet) vertical profile O3 algorithms that have been developed for the SBUV and follow on SBUV/2 instruments. This chapter describes the basis for the V8PRO implementation with emphasis on the changes from the Version 6 O3 profile algorithm (V6A) it is replacing. The V6A is described in *Bhartia et al. [1996]* and in the OMPS Nadir Profile ATBD [*Ball, 2002*]. Both the V6A and V8PRO use optimal estimation to generate maximum likelihood retrievals. See *Rodgers, [1976]* and *Rodgers, [1990]* for theoretical analysis of the properties of this class of retrievals, and *Meijer et al. [2006]* for applications to O3 profile estimation. This chapter also makes frequent references to the two previous chapters' descriptions of the physical basis of the measurements and the modeling techniques that are shared by the V8TOZ and the V8PRO.

The Version 8 vertical profile O3 algorithm (V8PRO) is the first new SBUV/2 algorithm since the Version 6 (V6A) in 1990. The V8PRO uses a new set of profiles for the *a priori* information leading to better estimates in the troposphere (where BUV measurements lack retrieval information) and to simplified comparisons of SBUV/2 and OMPS results to other measurement systems (in particular, the Umkehr ground-based O3 profile retrievals which now use the same set of *a prioris*). The V8PRO has improved total O3 retrievals from improved multiple scattering and cloud and reflectivity modeling. Some errors present in the V6A will be reduced. These include a correction for 2% errors from previously ignoring the gravity gradient with height and elimination of 0.5% errors from low fidelity bandpass modeling. The V8PRO is also designed to allow the use of more accurate external and climatological data, to adjust for changes in wavelength selection,

and to incorporate several *ad hoc* V6A improvements directly. Finally, the V8A is designed for expansion to perform retrievals for hyperspectral instruments, such as OMI, GOME-2 and the OMPS-NP. Some components of the initial V8PRO implementation were optimized for trend detection. These are modified for use in operations but the algorithm has the flexibility to make these changes.

The Solar Backscatter Ultraviolet instruments, SBUV on Nimbus 7 and SBUV/2s on NOAA-9, -11, -14, -16 and -17 -18, are nadir-viewing instruments that infer total column O<sub>3</sub> and the O<sub>3</sub> vertical profile by measuring sunlight scattered from the atmosphere in the ultraviolet spectrum. *Heath et al. [1975]* describes the SBUV flown on Nimbus-7. *Frederick et al. [1986]*, and *Hilsenrath et al. [1995]* describe the follow-on SBUV/2 instruments flown on the NOAA series of spacecraft.

The instruments are all of similar design; nadir-viewing double-grating monochromators of the Ebert-Fastie type. The instruments step through 12 wavelengths in sequence over 24 seconds, while viewing the Earth in the fixed nadir direction with an instantaneous field of view (IFOV) on the ground of approximately 180 km by 180 km. To account for the change in the scene-reflectivity due to the motion of the satellite during the course of a scan, a separate co-aligned filter photometer (centered at 343 nm on SBUV; 380 nm on SBUV/2) makes 12 measurements concurrent with the 12 monochromator measurements. Each sequence of measurements ends with an 8 second retrace, producing a complete set of measurements every 32 seconds on the daylight portions of an orbit.

The OMPS-NP and OMPS-NM continue this set of measurements with instruments using two-dimensional CCD arrays to obtain spectral measurements from 250 nm to 380 nm with approximately 0.4 nm sampling and 1.1-nm full-width half maximum bandpasses. The instruments are described in *Dittman et al. 2002*.

The instruments are flown in polar orbits to obtain global coverage. Since the BUV O<sub>3</sub> measurements rely on backscattered solar radiation, data are only taken on the dayside of each orbit. There are about 14 orbits per day with 26° of longitudinal separation at the equator. Unfortunately, the early NOAA polar orbiting satellites are not sun-synchronous. For example, the NOAA-11 equator crossing times drifted from 1:30 pm (measurements at 30° solar zenith angle or so at the equator) at the beginning of 1989 to 5:00 pm by the end of 1995 (measurements at 70° solar zenith angle). As the orbit drifts, the terminator crossing location moves to lower latitudes and coverage decreases. The OMPS instruments are on platforms with well-controlled orbits maintained close to 1:30 PM Equator crossing times.

Ozone profiles and total column amounts are derived from the ratio of the observed backscattered spectral radiance to the incoming solar spectral irradiance. This ratio is referred to as the backscattered top-of-atmosphere albedo (TOAA) or top-of-atmosphere reflectance. The only difference in the optical components between the radiance and irradiance observations is the instrument diffuser used to make the solar irradiance measurement; the remaining optical components are identical. Therefore, a change in the diffuser reflectivity will result in an apparent trend in O<sub>3</sub>. This is the key

calibration component for the BUV instruments. See *Hilsenrath et al. [1995]* for a longer discussion.

The spectral resolutions for SBUV(/2) and OMPS double monochromators are all approximately 1.1 nm, full-width at half-maximum (FWHM). The wavelength channels used for Nimbus 7 SBUV were at 256, 273, 283, 288, 292, 298, 302, 306, 312, 318, 331, and 340 nm. The wavelengths for NOAA-9 and the other NOAA SBUV/2 instruments were very similar except that the shortest channel was moved from 256 nm to 252 nm in order to avoid emission in the nitric oxide gamma band that contaminated the SBUV Channel 1 measurements. The OMPS hyperspectral measurements are converted to radiance irradiance ratios and these are linearly interpolated to give values at the target wavelength locations. The OMPS NP on S-NPP has been found to have a 0.015 nm amplitude annual variation in its wavelength scales related to thermal changes in the optical bench. The OMPS NP measurements are used for the eight shortest channels and the OMPS NM is used for the four longer ones.

Data from the 256 nm and 252 nm channels are not used in the V8PRO reprocessing for any of the instruments, but the algorithm allows for the use of this channel if desired, for example, in operational processing. The atmospheric O<sub>3</sub> absorption decreases by several orders of magnitude over the 252 nm to 340 nm wavelength range. The V8PRO uses a variable number of backscattered ultraviolet measurements depending on the solar zenith angle (SZA) of the observations to maintain its sensitivity to O<sub>3</sub> changes in the lower stratosphere. For small solar zenith angles (the sun high in the sky), only six wavelengths are used in the retrievals. They are at 273 nm, 283 nm, 288 nm, 292 nm, 298 nm, and 302 nm. As the SZA increases the 306 nm, then 313 nm and finally the 318 nm channels are added to the retrieval.

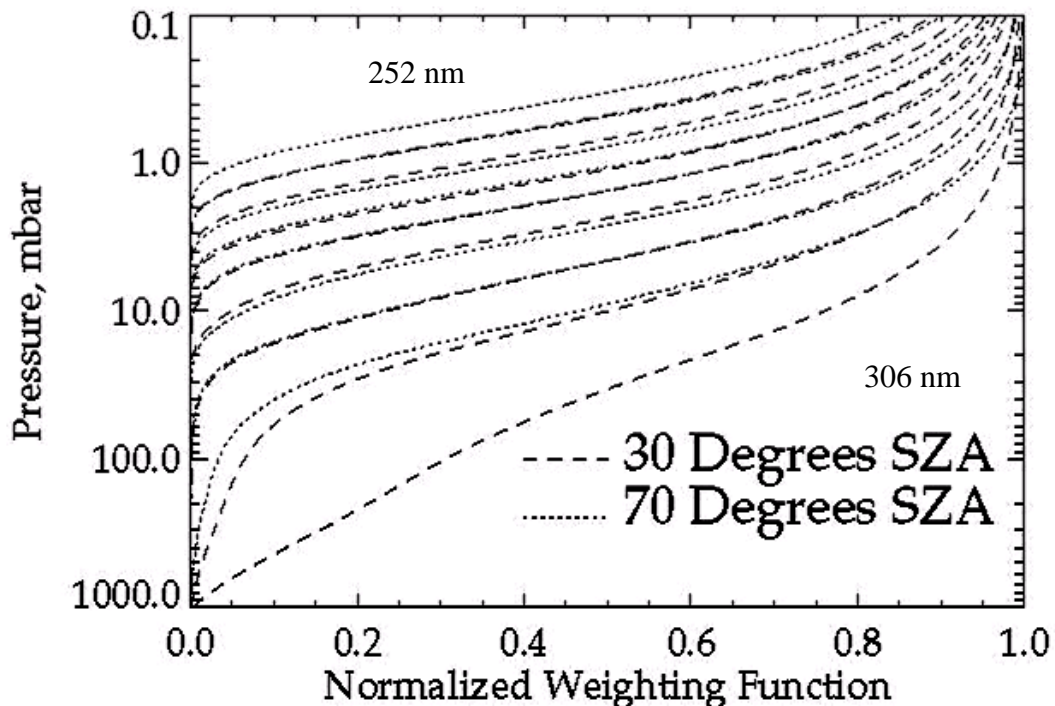


**Figure 2-3: Sample ozone weighting functions for the seven shortest SBUV/2 channels**

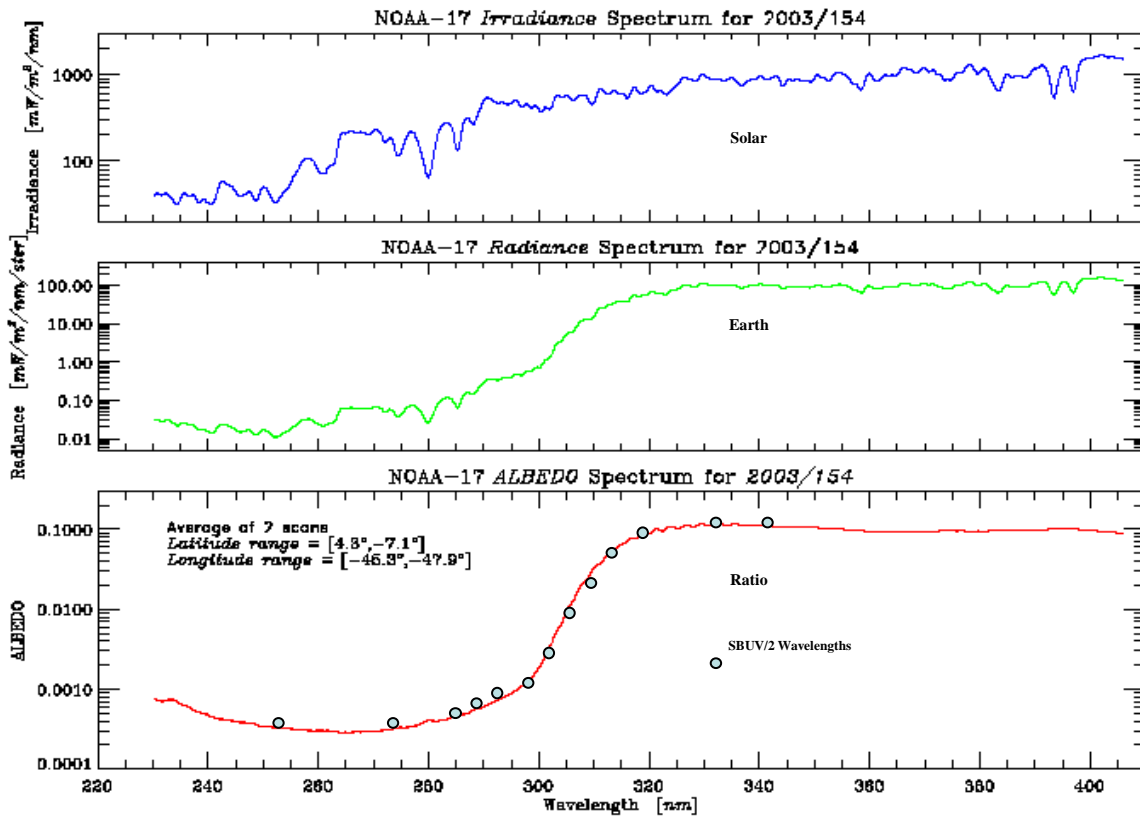
for two solar zenith angle. Wavelength results for each SZA case are short to long going from top to bottom.

Figure 2-3 shows the sensitivity of the profiling channels to unit O<sub>3</sub> changes at different heights. Because the shortest wavelengths are absorbed before penetrating very far, they only sense the O<sub>3</sub> amounts at the top of the atmosphere. When the sun is higher in the sky (lower SZA), the path length decreases and the photons penetrate farther into the atmosphere – compare the top two curves in Fig. 3-1.

### **2.3.2. Mathematical Description**

#### **Forward Model**

The UV radiances observed in the profiling wavelength channels (250 nm to 310 nm) vary by over four orders of magnitude. Sample Solar, Earth and TOAA measurements are shown in Fig. 3-2. The contributions to the shorter wavelength ( $\lambda < 290$  nm) channels are dominated by single scattered photons from the middle and upper stratosphere, while the longer wavelength channels ( $\lambda > 290$  nm) may have significant contributions from multiple scattering and surface and cloud reflectivity (MSR). See Fig. 1-2. for representative contribution functions for these wavelength ranges. Two different radiative transfer forward models are combined to represent the radiances. One uses a simple single scattering calculation while the other uses look up tables created with the TOMRAD forward model described in Section 2.2. The formulation of the single scattering model and the use of both models are described below.



**Figure 2-4: A Sample of Solar Irradiance (Top), Earth radiance (Middle), and Earth albedo (Bottom) measured by NOAA-17 SBUV/2.**

### Single Scattering Forward Model

The algorithm uses an internal forward model to estimate the single scattering components of the TOA. For an atmosphere containing only Rayleigh scatterers and  $O_3$ , for a wavelength  $\lambda$ , the optical depth in the atmosphere in the nadir direction, as a function of pressure,  $\tau_\lambda(p)$ , can be written as  $\tau_\lambda(p) = \int \alpha_\lambda(t(p'))x(p') + \beta_\lambda dp'$  where,  $x(p')$  is the derivative of the column  $O_3$  amount above a pressure  $p'$  [ $x(p) = dX(p)/dp$  where  $X(p)$  is the partial column of ozone from the top of the atmosphere down to pressure  $p$ ],  $\alpha_\lambda(t)$  is the  $O_3$  absorption coefficient at temperature  $t$ , and  $\beta_\lambda$  is the Rayleigh scattering coefficient at a wavelength  $\lambda$ .

At wavelengths below 290 nm, little solar radiation penetrates below 30 km, permitting surface, cloud, and aerosol effects to be ignored. Because radiation is scattered from a region of the atmosphere which is optically thin for scattering, multiple scattering effects may also be ignored. For such cases, the backscattered radiance intensity in Eq. (2.1) can be explicitly written to a high degree of accuracy as

$$R_\lambda = (1/4\pi)F_\lambda\beta_\lambda P(\cos\theta_0) \int \exp[-\int s(p)(\alpha_\lambda(t(p))x(p) + \beta_\lambda) dp'] dp \quad (3.1)$$

Where  $\theta_0$  is the solar zenith angle,  $s$  is the slant path factor (air mass factor),  $P$  is the Rayleigh phase function,  $F_\lambda$  is the solar flux, and  $p$  is pressure. The outer integral limits are the surface to the top of the atmosphere. The inner integral limits are pressure  $p$  to the top of the atmosphere. This expression for  $R_\lambda$  is commonly described as the single scattering radiance. The Rayleigh phase function,  $P(\cos\theta_0)$ , assuming a depolarization factor of 0.035 (Bates, 1984), can be written as

$$P(\cos \theta_0) = 0.7619 (1 + 0.937 \cos^2 \theta_0). \quad (3.2)$$

The slant path (air mass),  $s$ , for the SBUV/2 or OMPS nadir viewing geometry, can be approximated by  $1 + \sec(\theta_0)$  at low solar zenith angles ( $<60^\circ$ ), or by the Chapman (1931) function at moderate solar zenith angles ( $<80^\circ$ ). For solar zenith angles greater than  $80^\circ$ ,  $s$  must be treated as a function of  $p$ , calculated by ray-tracing. The slant pass must also be modified to account for the increase in neutral atmosphere as a function of pressure increments with increasing height, that is, the gravity gradient. This increases the scatters by a factor of  $[1 + H(p)/R_e]^2$  where  $R_e$  is the radius of the Earth at a surface at 1 atmosphere and  $H(p)$  is the physical height the layer at pressure  $p$  is above this surface. We will work with the top of atmosphere albedos (TOAA)  $I = R/F$ .

The algorithm computes the single scattered albedos and the corresponding Jacobians of partial derivatives with respect to layer  $O_3$  amounts for given UV channels by using a double discretization of Eq. (3.1) in atmospheric pressure and wavelength bandpass. The discretization in pressures represents the atmosphere by using 81 pressure layers with constant logarithmic spacing. Approximation of the atmosphere by using the pressure layers transforms the integral in Eq. 3.1 into a discrete sum with  $x(p)$  transformed into a corresponding discrete set of  $O_3$  layer amounts, and  $t(p)$  into a discrete set of mean layer temperature values. The partial derivatives of  $I$  with respect to  $O_3$  layer amounts can be efficiently computed by multiplying the component results for  $I$  by the appropriate  $-\alpha$  values and computing the appropriate sums.

The second discretization concerns the representation of the wavelength channels 1.1-nm bandpasses. These are modeled by using a discrete set of 21 wavelengths spaced at 0.1 nm intervals around each bandpass center, multiplying the calculated  $I_\lambda$  for each wavelength by the relative bandpass contribution, and summing to provide the estimate of the full channel. Results using finer spacing and additional weighting to model solar variations produced small additional improvements.

### Multiple Scattering Forward Model

The multiple-scattering forward model used in the V8PRO is the same radiative transfer forward model described in Section 2.2, namely, TOMRAD. Again it is used to create look-up tables of radiances and Jacobians. In this case, the look-up tables give the relative changes between the MSR results and the single scattering results. That is, the tables give the ratio of full multiple scattering and reflectivity simulations and partial derivatives to corresponding single scattering ones. This means that they give the values to transform single scattering albedos or Jacobians computed by the internal forward model into full multiple scattering and reflectivity estimates. Additional tables with the sensitivity of the Jacobian tables to  $O_3$  layer changes allow the algorithm to

track changes in the partial derivatives even when the iterations of the O<sub>3</sub> profile solution, described in the next section, move away from the standard profiles used to generate the tables.

### Spectroscopic Constants

The same data sets are used for the O<sub>3</sub> cross-sections and Rayleigh scattering as are described in Section 2.2.1.

### 2.3.3. Retrieval Algorithm

The retrieval algorithm uses a maximum likelihood retrieval combining *a priori* O<sub>3</sub> profile information with the BUUV measurements. The longer channel measurements are used to provide an initial total O<sub>3</sub> estimate (used only to generate the first guess) and a cloud/surface reflectivity estimate (adjusted for photometer variations but fixed for the retrieval). The measurement vector is represented by  $Y_M$  and contains the natural logarithm of the TOAAs for the shorter channels (the number of channels is varied with solar zenith angle and total O<sub>3</sub>); the unknown O<sub>3</sub> profile is represented by a vector  $X$  and its components are the values for layer O<sub>3</sub> content in Dobson Units for each of 21 pressure layers; and the corresponding 21-layer *a priori* O<sub>3</sub> profile is represented by a vector  $X_A$  as defined in the next section. The 21 layers are defined by 21 pressure levels at

$$P = [ 1.0, 0.631, 0.398, 0.251, 0.158, \\ 0.1, 0.0631, 0.0398, 0.0251, 0.0158, \\ 0.01, 0.00631, 0.00398, 0.00251, 0.00158, \\ 0.001, 0.000631, 0.000398, 0.000251, 0.000158, 0.0001 ] \text{ Atm.}$$

That is, with 5 layers per decade of pressure or approximately 3-KM spacing, except for the last layer; it extends to the top of the atmosphere. Some calculations are performed on finer layers with a total of 81 sublayers (20 per decade or pressure) each approximately 0.8-KM thick. The following sections describe the components of the maximum likelihood retrieval, namely: the *a priori* O<sub>3</sub> profile data set, the *a priori* and measurement covariance matrices, the forward model linearization and Jacobian construction, and the iteration and its stopping criteria.

### 2.3.4. Version 8 Algorithm A Priori Profiles

The *a priori* profile database was created from 15 years (1988-2002) of ozonesonde measurements and SAGE (Version 6.1) and/or UARS-MLS (Version 5) data. Over 23,400 sondes from 1988-2002 were used in producing this climatology. The data were "filtered", *i.e.*, obvious bad data points were removed. Balloons that burst below 250 hPa were discarded. Data from bouncing balloons were sorted by pressure. Note: No total O<sub>3</sub> correction factor (TOMS or Dobson) filtering was used. The stations were weighted equally for each band so that we do not introduce any longitudinal biases (*e.g.*, Resolute and Nyalesund have equal weights in December even though Nyalesund has three times as many sondes as Resolute for that month). The SAGE

data was also "filtered" for bad retrievals. Average profiles from ozonesondes and SAGE are merged over a 4-km range with the sonde weight decreasing from 80 to 60 to 40 to 20% and the SAGE weight increasing correspondingly. The covariance matrices associated with this data set are available but as noted below, artificial covariance matrices are used in generating the BUW operational and reprocessed retrieval products.

The *a priori* profile data set is the same as the 3-dimensional standard profile data set for the V8TOZ. It gives the climatological O<sub>3</sub> profile averages for 18 10° latitude bands and 12 months. The lowest layer from the *a priori* program will differ from that used in the retrieval if the surface pressure is not 1 atmosphere. These profiles are used to determine the discrete *a priori* O<sub>3</sub> profile used in a specific retrieval by linear interpolation in latitude and day. This discrete O<sub>3</sub> profile is designated by a vector  $X_A$  whose components are layer amounts in Dobson Units. Another data file with terrain heights as a function of latitude and longitude is used to generate the surface pressure for given latitude and longitude, and the lowest layers are truncated as appropriate.

### 2.3.5 Retrieval Formulation

The retrieval formulation begins with a linearization of the discretized forward model about a first guess for the O<sub>3</sub> profile,  $X_0$ . This first guess is from a total O<sub>3</sub> and latitude interpolation of the 21 standard profiles used in the V8TOZ. In addition to the O<sub>3</sub> profiles, look up tables contain the forward model adjustments to convert single scattering estimate to the full multiple scattering and reflectivity TOAA values. The  $Y_0$  [TOAA forward model estimates of  $\log(R/F)$ ] are found by using the single scattering model applied to  $X_0$  for the current measurements viewing conditions and adjusting them to calculate the full multiple scattering values by using the factors from the look-up table tables (with the same total O<sub>3</sub> and latitude interpolations). The linearization is given by

$$Y = Y_n + K_n (X - X_n) \quad n=0,1,\dots \quad (3.3)$$

Where  $Y_n$  is the forward model estimate after iteration  $n$ ,  $X_n$  is the O<sub>3</sub> profile estimate after iteration  $n$ , and  $K_n$  is the Jacobian matrix of partial derivatives of the components of  $Y$  with respect to the components of  $X$  ( $\partial y_i / \partial x_j$  where individual  $y_i$  and  $x_j$  represent  $\log$  of TOAA for a BUW channel and an O<sub>3</sub> pressure layer amount, respectively) evaluated at  $X_n$ . The partial derivative coefficients in  $K$  are calculated by using the O<sub>3</sub> profile for the previous iteration ( $X_n$ ) and constitute the weighting function. They measure the sensitivity of the radiance at a particular wavelength to changes in O<sub>3</sub> in the different layers in the profile.

The iterative solution proceeds by generating the optimal estimation (maximum likelihood) solution for the current linearized problem by using the following calculation

$$X_{n+1} = X_A + S_A K^T [K_n S_A K_n^T + S_M]^{-1} [Y_M - Y_n) - K_n (X_A - X_n)] \quad (3.4)$$

Where  $X_n$  is the discrete O<sub>3</sub> profile from iteration n,  $X_{n+1}$  is the new discrete O<sub>3</sub> profile estimate,  $X_A$  is the discrete *a priori* O<sub>3</sub> profile as described in Section 3.3.1,  $Y_M$  is the vector of measurements from the SBUV/2 or OMPS NP for the profiling channels;  $Y_n$  and  $K_n$  are the forward model and Jacobian estimates for an atmosphere containing layer O<sub>3</sub> amounts,  $X_n$ ; and  $S_A$  and  $S_M$  are the *a priori* and measurement covariance matrices, respectively. The algorithm uses the size of the RMS change in X from one iteration to the next as a stopping criterion.

The theoretical algorithm does not place any restrictions on the covariance matrices  $S_A$  and  $S_M$  except that they should be non-negative definite with the proper dimensions. In practice, the V8PRO uses an artificial  $S_A$  matrix constructed by specifying the diagonal to give a constant percent variability for the O<sub>3</sub> in each layer and then using a scale height correlation to specify the off diagonal values. The  $S_M$  matrix is taken to be a diagonal matrix as the SBUV/2 and OMPS show little correlation in noise between channels.

For reprocessing, the *a priori* covariance used in the maximum likelihood retrieval is an artificial construct as follows: the diagonal elements correspond to 50% variance and the non-diagonal covariance elements fall off with a correlation length of twelve fine layers (approximately 10 KM). The measurement covariance,  $S_M$ , is a multiple of the identity matrix and the diagonal entries correspond to radiance errors of 1% in each channel. For operational processing this is increased to 2%. We are considering assigning more realistic noise levels to these entries as functions of instrument performance in the different channels and at different signal levels.

The computation of the Jacobian matrix, K, is performed in three steps at each iteration. First the internal single scattering model is used to estimate the partial derivatives for the single scattering radiances, second multiple scattering adjustments to the partial from the previous iteration are updated with the table partial sensitivities and the change in the retrieved profile from the last iteration, finally, the multiple scattering partial adjustments are applied in a first order (linear) expansion to generate the new full multiple scattering and reflectivity Jacobian from the one for the previous iteration.

### 2.3.6. Averaging Kernels

Unlike the V6 profile retrieval algorithm, the V8a has a true separation of the *a priori* and first guess. This simplifies averaging kernel analysis. Averaging kernels are an algebraic construct of the linearized problem given in Eq. (3.4). One can manipulate the equation to give an expression involving the Averaging Kernel Matrix, A. This produces the solution in terms of an impulse-response formulation. Specifically,

$$X_R = X_A + A (X_T - X_A) = (I-A) X_A + A X_T \quad (3.5)$$

where  $X_T$  is the true profile,  $X_A$  is the *a priori* O<sub>3</sub> profile, and  $X_R$  is the retrieved O<sub>3</sub> profile.

If one considers how the retrieved profile responds to a unit change in a single layer of the true profile, then the impulse response interpretation of the averaging kernel is clear. These retrieval impulses to truth deviations from the *a priori* profile can be plotted as profile responses to changes at a specified level.

Figures 3.3a, 3.3b and 3.3c give some sample averaging kernel plots to help to describe the V8PRO retrieval capabilities. They show Averaging Kernels (AK) (for fractional changes in O3 layer amounts) at 15 middle and upper stratospheric pressure levels. The short horizontal lines on the right side of the graph show the pressure levels and point to the corresponding AK. The horizontal and AK lines' styles correspond. In general, the (fractional) variation in the mixing ratio reported by BUJ retrievals at a given pressure level is a weighted average of the (fractional) variation of the real mixing ratio at surrounding altitudes, relative to the *a priori* profile. Since the V8PRO *a priori* profiles have no inter-annual variation, the AKs also show how the algorithm would smooth a long-term trend in O3 mixing ratio. Note, however, that individual BUJ profiles usually have structures that are finer than those implied by the AKs; these structures come from the assumed *a priori* profile, rather than from the measurements themselves.

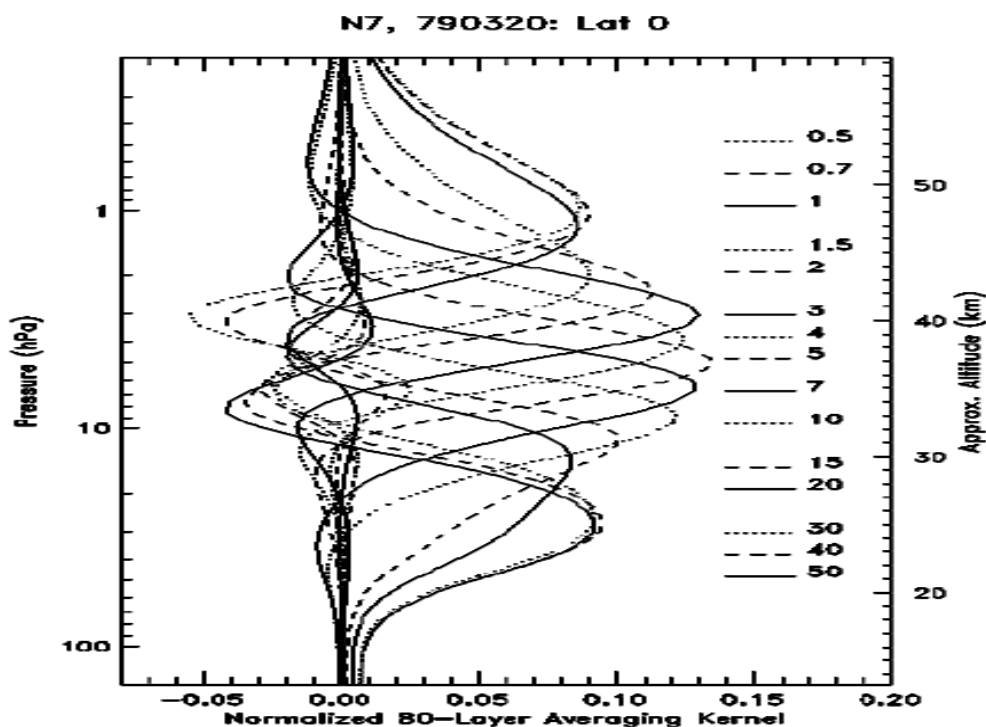


Figure 2-5a: Averaging kernel as fractional layer changes for an equatorial profile and viewing condition.

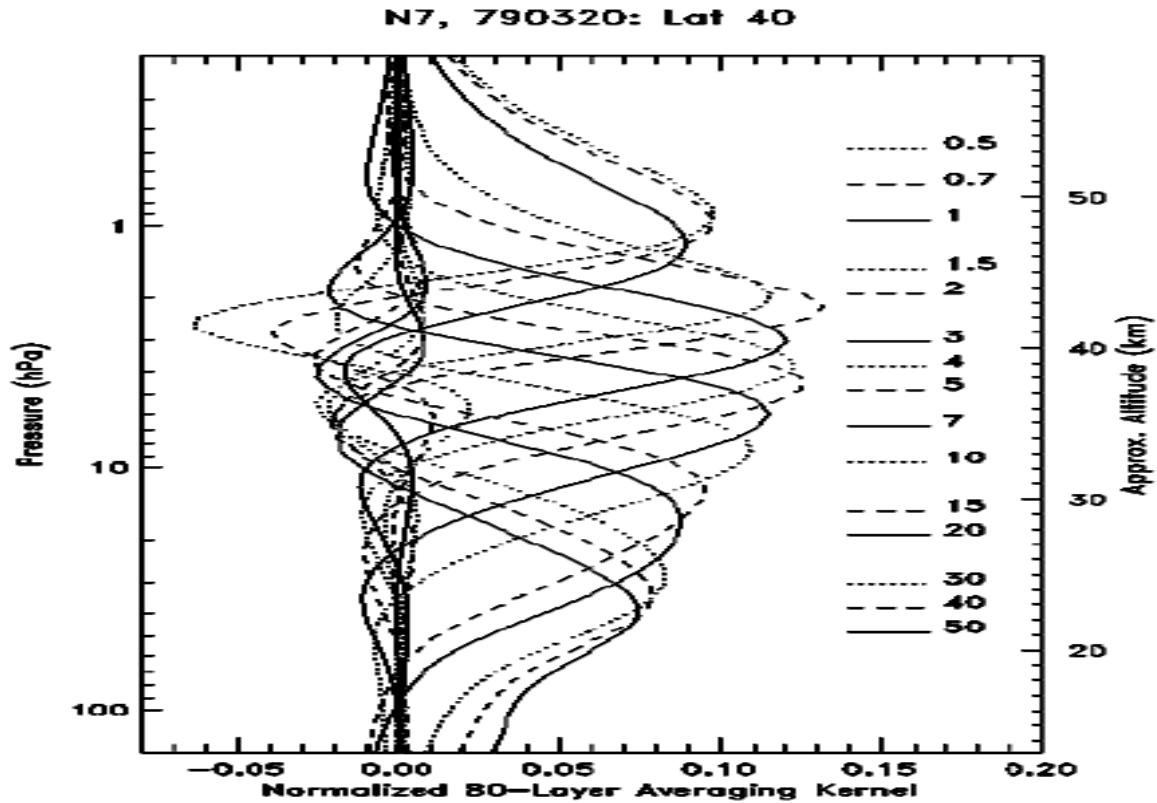


Figure 2-5b: Averaging kernel as fractional layer changes for a mid-latitude profile and viewing condition.

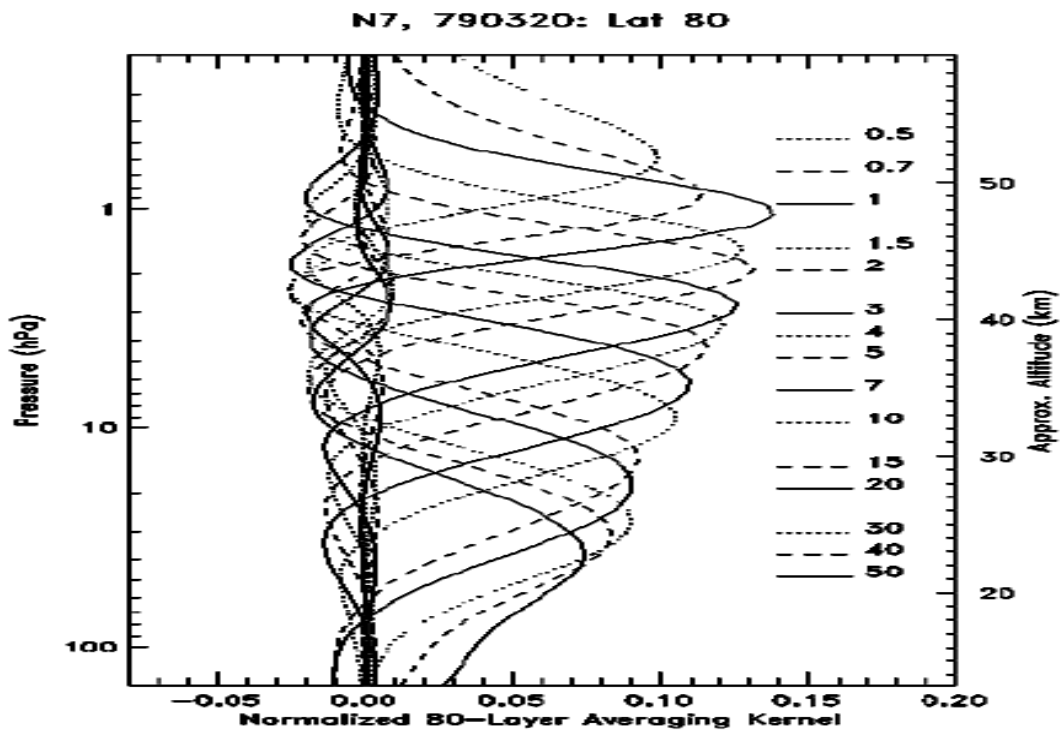


Figure 2-5c: Averaging kernels as fractional layer changes for a high latitude profile and viewing condition.

Figure 2-5a shows typical AKs at the equator. The AKs show best resolution of ~6 km near 3 hPa, degrading to ~10 km at 1 and 20 hPa. Outside this range the retrieved profiles have little information. For example, the (fractional) variation in O<sub>3</sub> mixing ratio seen at 0.5 hPa actually represents the (fractional) variation from the region around 1 hPa, and the variation around 50 hPa represents the variation from around 30 hPa.

Figure 2-5b shows typical AKs for March at 40N latitude. At this latitude the 50 hPa AK does capture some of the atmospheric variation, albeit with a FWHM resolution of ~11 km. In general, the upper AKs get progressively better as the solar zenith angle increases, and the lower AKs become better as the O<sub>3</sub> density peak drops in altitude. Figure 3.3c shows typical AKs for March at 80N latitude. One can see the improvement in AKs for the upper portions of the profile, especially the 0.5, 0.7, 1, and 1.5 hPa AKs, in capturing the atmospheric variation more accurately than in Figs. 2 and 1, with better resolution of ~6 km at 0.7 hPa.

The AK results presented here use the  $S_A$  and  $S_M$  covariance matrices applied for the reprocessed product retrievals. The operational retrievals use an  $S_M$  matrix with larger entries to allow for the greater uncertainty in the operational calibration. The averaging kernels for the operational implementation are slightly broader than those shown here.

### 2.3.7 Error Analysis

The V8PRO combines backscattered ultraviolet measurements and *a priori* profile information in a maximum likelihood retrieval placing it in the same class of retrievals as V6A described in *Bhartia et al. [1996]*. The following list gives an overview of how errors will be reduced:

1. The V8PRO has new set of *a priori* profiles varying by month and latitude leading to better estimates in the troposphere (where BUUV methods lack retrieval information) and allowing simplified comparisons of SBUV/2 and OMPS results to other measurement systems (in particular, to Umkehr ground-based O<sub>3</sub> profile retrievals which use the same *a priori* data set).
2. The V8PRO has a true separation of the *a priori* and first guess. This simplifies averaging kernel analysis. Examples and further information on the smoothing errors were provided above.
3. The V8PRO has improved multiple scattering and cloud and reflectivity forward model estimates. These corrections are updated as the algorithm iterates toward a solution.
4. Some errors present in the V6A will be reduced or corrected. These include a reduction of errors on the order of 0.5% down to 0.1% by improved fidelity in the bandpass modeling, and a reduction in errors from inelastic scattering by including average adjustments for each channel for these effects.
5. The V8PRO incorporates several *ad hoc* V6A improvements directly. These include better modeling of the effects of the gravity gradient, better representation of atmospheric temperature influences on O<sub>3</sub> absorption, and better corrections for wavelength grating position errors.
6. The V8PRO uses improved terrain height information compared to the V6A and gives profiles relative to a better climatology of surface pressure.
7. The V8PRO is designed to allow the use of more accurate external and climatological data (*e.g.*, snow and ice fields) and to allow simpler adjustments for changes in wavelength selection and calibration.

8. Finally, the V8PRO is designed for expansion to perform retrievals for hyperspectral instruments, such as OMI, GOME-2 and the Nadir Profiler in OMPS so future comparisons will be simplified.

The V8PRO uses the same profiling wavelengths and measurements as those used by the V6A and both algorithms are maximum likelihood retrievals. This means that the retrieval responses to measurement noise and bias will be similar if similar  $S_M$  and  $S_A$  matrices are used. There is a fundamental difference in their use or non-use of total ozone information for the ozone profile retrievals. The V6A uses the total ozone estimate for the scan sequence as a constraint on the maximum likelihood retrieval. The V8PRO has no such constraint so the total profile ozone is controlled by the profile wavelength information and the *a priori* profile amounts. This means that the best total ozone estimates from the V8TOZ may differ from the total of the profile retrievals. The profile total will have less sensitivity to real tropospheric ozone changes, but they will also have less sensitivity to tropospheric aerosol effects which are difficult to model.

### **Forward Model Errors**

The V8PRO has several refinements in this area. The single and multiple scattering forward model applications for the V8PRO are improved relative to V6, and the *a priori* climatological  $O_3$  data are from a more complete set of profiles with improved information on seasonal and latitudinal variations of tropospheric ozone. The new *a priori* data set leads to improvements in the retrievals in the troposphere where the BUUV retrievals lack information and to easier interpretation of the source of information in the retrieved profiles. This means that the radiances attributed to the stratosphere are more accurate.

The internal single scattering forward model has itself been made more accurate as follows: It now uses a discrete sum of monochromatic results to represent the instrument bandpass and incorporates a temperature profile in the  $O_3$  cross-section calculation (instead of using “effective” cross sections without any pressure dependence as was the case for the V6A); and it corrects for the gravity gradient in scatterers with height.

The V6 profile algorithm made an initial adjustment to the radiances to account for MSR differences with the single scattering model and then proceeded with only single scattering calculations as it iterated to a solution. The V8PRO has improved multiple scattering and cloud and reflectivity modeling by the use of the MSR tables of corrections and Jacobians. These are used to update the MSR versus single scatter adjustments after each iteration in the retrieval process. In addition, the average effects of inelastic Raman scattering (RRS) are computed for each profiling wavelength and a set of adjustments are used to represent these contributions to first order. Both forward models use a new data based of terrain height (surface pressure) with improvements in both its accuracy and spatial resolution.

### **Inverse Model Errors**

The discretization of the atmosphere in 0.8-KM layers and the discretization of the bandpass at 0.1-nm wavelength intervals were chosen to reduce modeling errors from these sources to 0.1% levels. The smoothing error of the retrievals (inherent in any remote-sensing maximum-

likelihood inversion) can be observed in the Averaging Kernel results in the previous section. As noted, resolution varies from 6 KM in the middle/upper stratosphere to 20 KM in the troposphere.

### Temperature

The current implementations use a set of climatological temperature profiles which capture the main seasonal and latitudinal features of the temperature variations. If improved estimates, *e.g.*, from current forecasts or assimilations are available, then these can be used. By noticing that the radiances in Eq. 3.1 depend on the product of the ozone amount at pressure  $p$ ,  $x(p)$  multiplied by the ozone cross section as a function of the temperature at pressure  $p$ ,  $\alpha(t(p))$ , one can switch between partial derivatives with respect to  $x$  to those with respect to  $t$  by using the chain rule. Specifically,

$$\partial y_i / \partial t_j = \partial y_i / \partial x_j [x_j / \alpha_j] d\alpha_j / dt_j \quad (3.6)$$

for channel  $i$  and layer  $j$ .

#### 2.3.8. Instrumental Errors

This section investigates the response of the profile retrievals to errors in the measurements. It begins by showing results from sensitivity calculations for wavelength-independent and wavelength-dependent errors. A full day of reprocessing retrievals for NOAA-17 SBUV/2 for September 1, 2006 is used as the baseline. These profiles are compared to those from additional runs of the same day with perturbations to the measurements. The sensitivity results are followed by estimates of the size and occurrence of a variety of instrument and measurement errors including calibration uncertainties, stray light and wavelength scales.

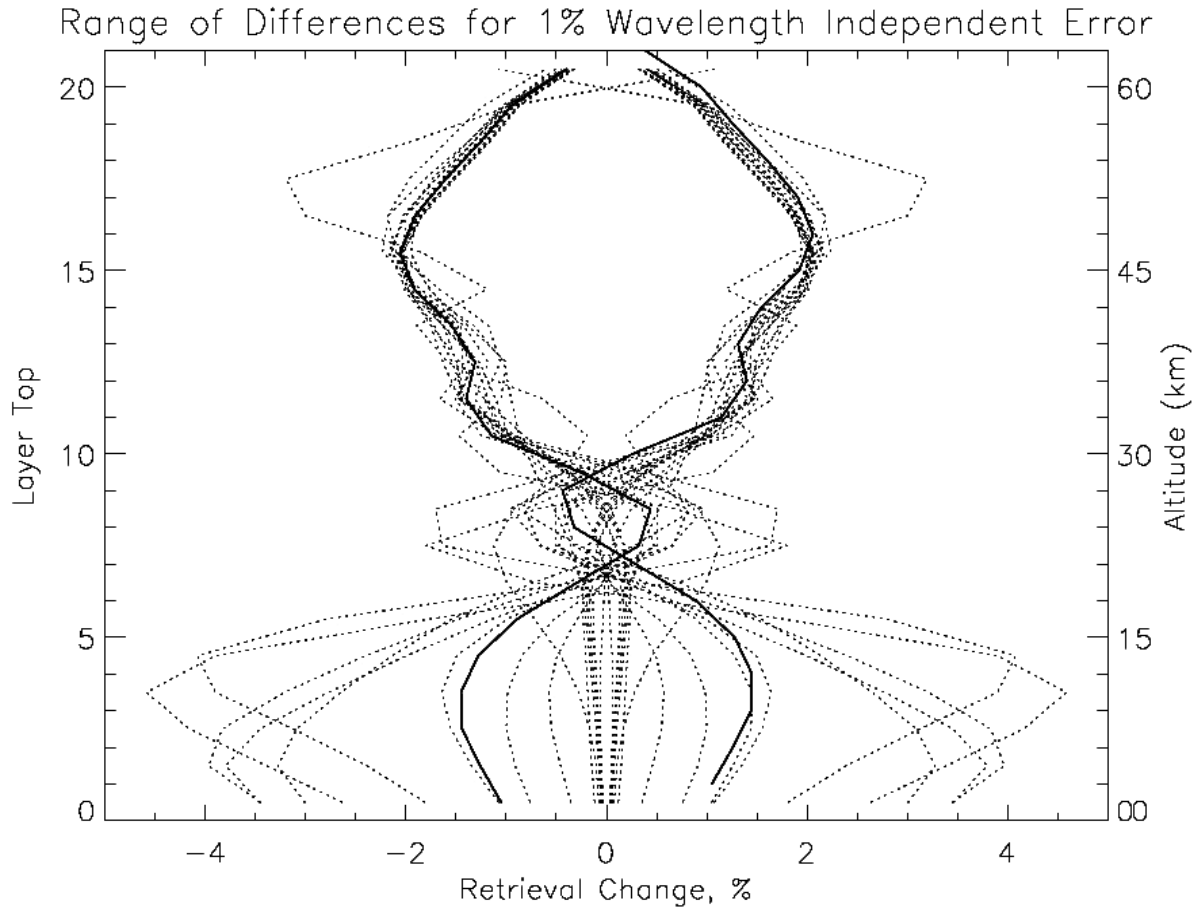


**Figure 2-6: Difference in retrieval responses for  $\pm 1\%$  uniform measurement errors at all profiling wavelengths at 16 latitudes (every  $10^\circ$  from 75S to 75N)**

Figure 2-6 shows the effects of a uniform shift in the calibration of all the profile wavelength measurement channels. The thick solid line gives the paired results for 45N latitude when all channels are increased by 1% or all channels are decreased by 1%. The dotted lines give the paired results for other the full range of latitudes covered by the SBUV/2 or OMPS NP, 80S to 80N. The retrieval algorithm interprets a 1% increase in the radiances at all profiling channels at 45N as a decrease in the middle and upper stratospheric ozone amounts of approximately 2%, little change in the lower stratosphere, and an increase in the tropospheric ozone amounts of 1%.

Figure 2-7 shows the effects of -0.5% shifts in individual channels for six profiling wavelength channels – 273 nm, 283 nm, 288 nm, 292 nm, 298 nm and 302 nm — for a retrieval at 45N latitude. The six curves go from the shortest channel to the longest in the following order; Thick Solid, Thick Dotted, Thick Dashed, Thin Solid, Thin Dotted, Thin Dashed. In general, the larger retrieval differences are found higher in the atmosphere for the shorter wavelengths and lower in the atmosphere for the longer ones. These features will follow the pattern of the contribution function shown in Fig 3-1, moving higher with increases in SZA or ozone amounts. The  $S_A$  and  $S_M$  matrices were in their reprocessing configuration for these sensitivity tests.

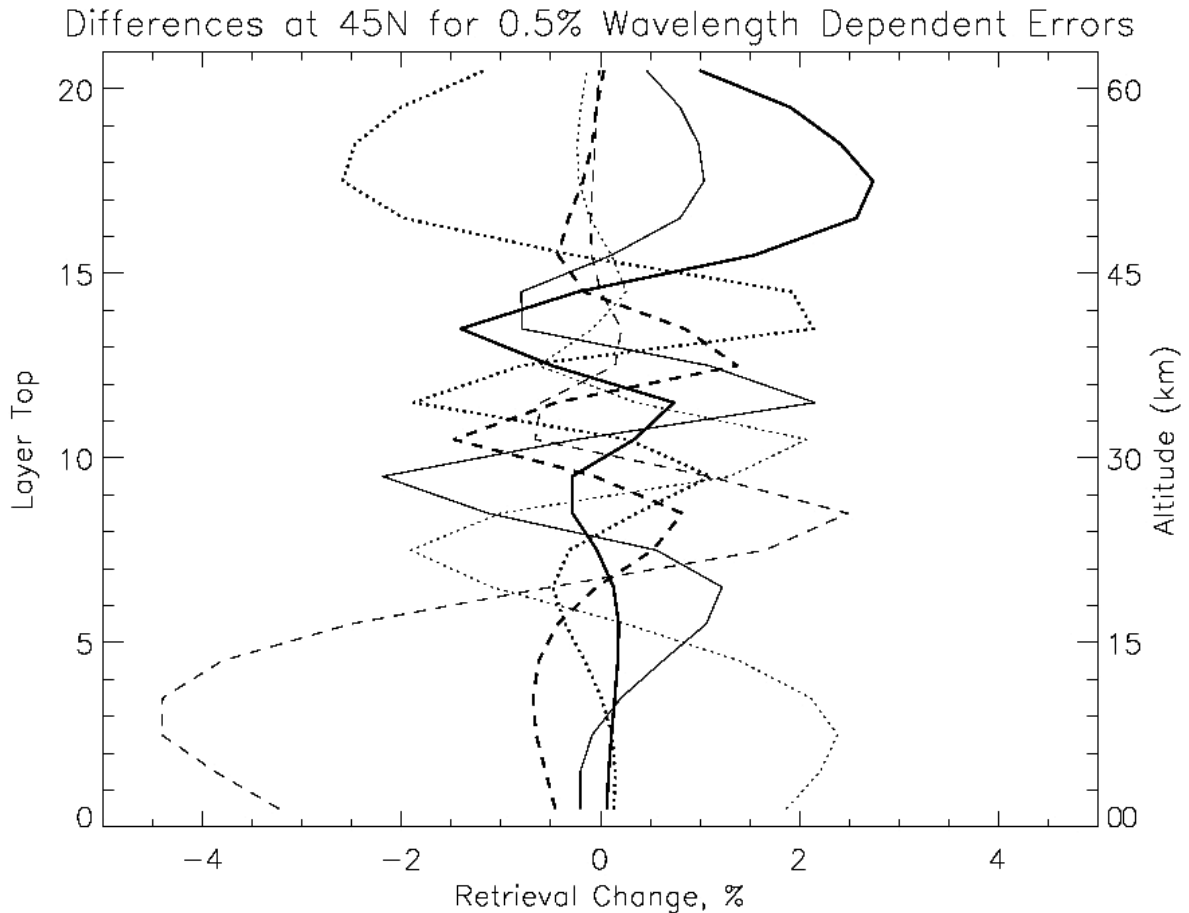


**Figure 2-7: Difference in retrieval response for -0.5% measurement errors at individual profile wavelengths – 273, 283, 288, 292, 298 and 302-nm channels for the 273-nm to 302-nm channels at 45N latitude.**

### Radiometric Calibration

The measurement errors modeled in Figs. 3-4 & 3-5 were chosen because they are representative of the types of uncertainties expected in the TOAA calibration for the SBUV/2 instruments, that is, errors in the overall calibration of all the channels combined with errors in the relative calibration of individual channels. Details on the calibration of the SBUV/2 instruments are beyond the scope of this ATBD. Material on the methods for maintaining this

calibration and estimates of the success of their application can be found in the following articles and their references: *Herman et al. [1991]*, *Bhartia et al. [1995]*, *Hilsenrath et al. [1995]*, *Cebula and DeLand [1998]*, *Flynn et al. [2000]*, *Huang et al. [2003]*, *Deland et al. [2002]*, and *Flynn et al. [2006]*. The OMPS instruments have better designs to maintain their calibration. A reference on the results for OMPS from the first two years was provided in the first chapter.

### Stray Light

The UV measurements are affected by two types of stray light – in band stray light (IBSL) and out-of-band stray light (OBSL). Instruments behaviors range from very small stray light errors for both of these sources (*e.g.*, NOAA-9 SBUV/2) to significant impact from both (*e.g.* NOAA-17 SBUV/2).

Figure 3-6 shows evidence of OBSL for the NOAA-17 SBUV/2 from ground measurements of sun on the diffuser. The symbols show the actual measurements at the discrete SBUV/2 wavelengths. The solid line gives an extrapolation using ozone retrieved from the longer wavelength measurements to predict the true signal for the shorter wavelengths. The atmosphere is a very strong filter below 290 nm, so the true signals should be below the instrument noise level (given by the horizontal line). The measurements for the shortest five wavelengths all show significant OBSL. Empirical methods using correlations between longer channel reflectivity variations and shorter channel stray light have been used to devise models and corrections. After applying these corrections, systematic errors are removed, but some scene- and SZA-dependent errors at the 0.5% level remain.

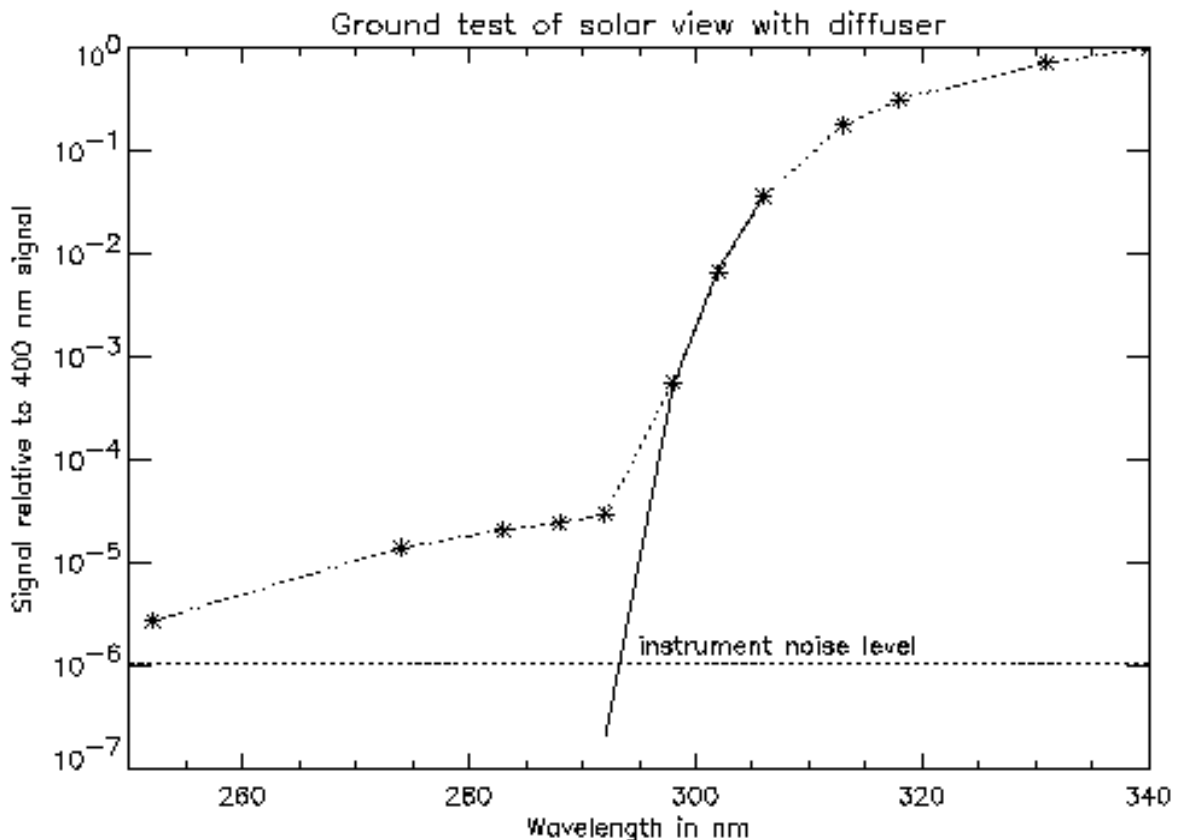
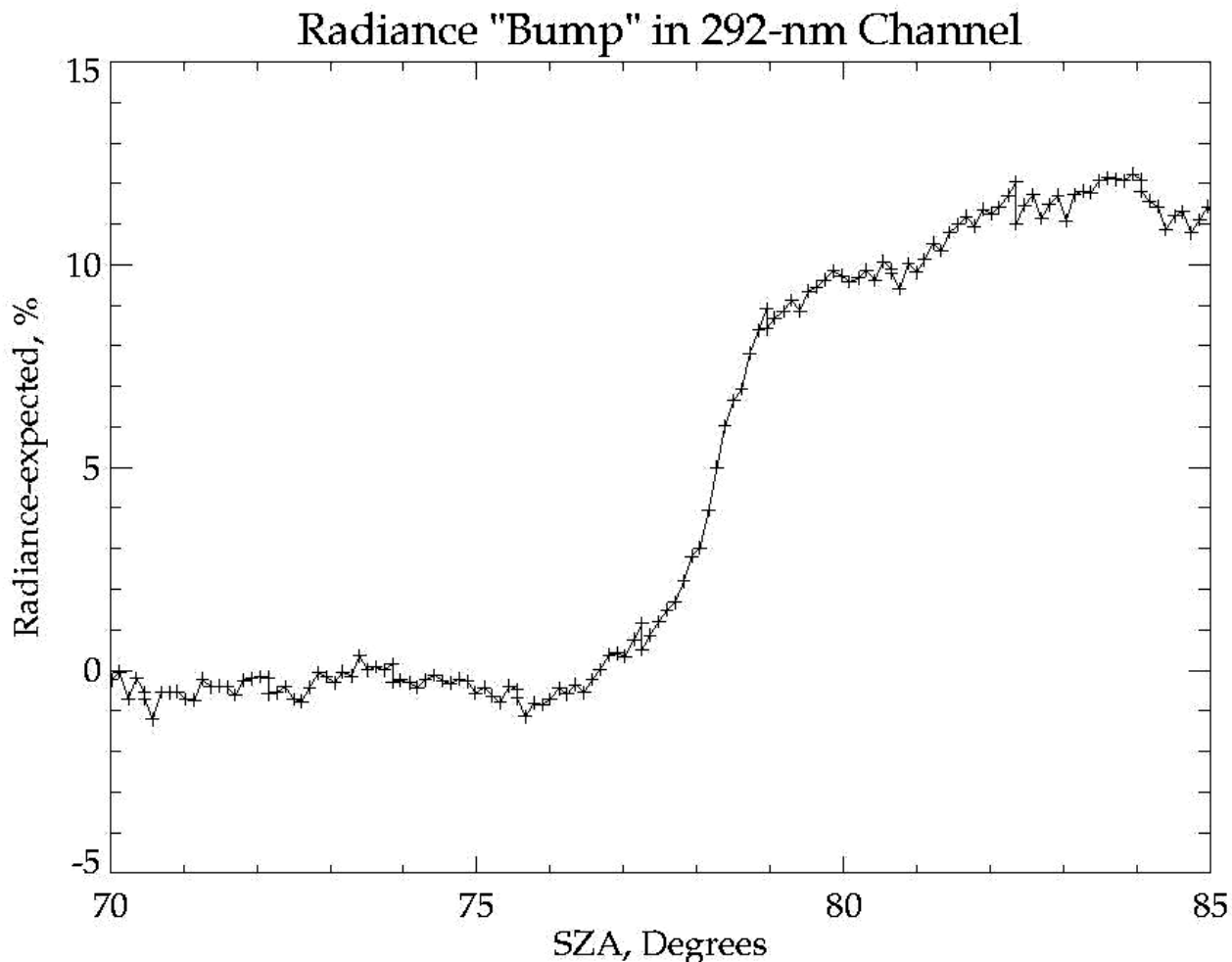


Figure 2-8: Out-of-Band Stray Light for NOAA-17 SBUV/2 observed in Ground Test.

Figure 3-7 shows evidence of IBSL for NOAA-17 SBUV/2 in the 292-nm channel. The presence of this “bump” is exposed by using a linear extrapolation of the radiances versus SZA for the 70° to 75° range and subtracting it from the data. The 10% radiance error at 292 nm is caused by sunlight scattered from the instrument or spacecraft into the entrance aperture. Fortunately, the phenomenon is limited to high SZAs and predictable satellite azimuth angles. Unfortunately, when it occurs it affects most of the profiling wavelengths, and is seen on the SBUV/2 instruments on NOAA-14, -17 and -18, although only at high SZA and only in one hemisphere for any orbit.



**Figure 2-9: Onset of In-band Stray Light at 77° SZA as Seen in NOAA-17**

The measurements affected by these two stray light errors are either corrected to the 0.5% or better level (in the case of OBSL) or flagged as bad retrievals (in the case of IBSL). A correction to bring the errors for the IBSL case below the 0.5% level is under development.

The OMPS NP and NM also have stray light contributions to the measurements. These were well-characterized in the laboratory and have been used to create measurement based correction models. These have been implemented in the Level 1 (SDR) OMPS processing.

## Wavelength Scale and Bandpass

Measurements at lamp or solar lines can also be used to track the wavelength scale and monitor the bandpass shape. Figure 3-8 shows the results of continuous scan mode measurements (taken every 0.15 nm) across four Hg-Lamp lines. This data is analyzed to estimate the line centers as functions of the monochromator grating positions providing accurate characterization of sensor wavelength scale at the 0.01 nm level. The nearly-triangular, 1.1-nm instrument bandpass is also confirmed. These characterizations reduce the errors from these sources to the 0.1% levels. (Figure 3-8 is reproduced from *DeLand et al [2002]*.)

SSAI-2015-

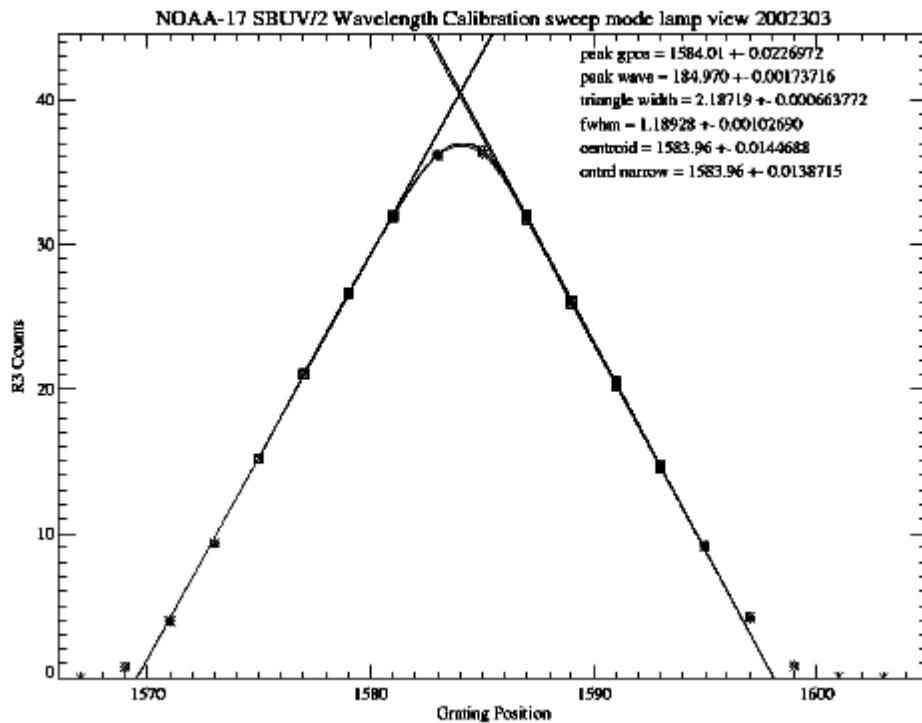


**Figure 2-10: Signal Levels across an Hg-Lamp Line from Continuous Scan**

The OMPS NP and OMPS NM have wavelength scale variations related to changes in the thermal environments. The OMPS NM located at the side of the instrument structure shows intra-orbit variations with an amplitude of 0.02 nm. Because of the hyperspectral nature of the measurements, we are able to estimate these shifts on a spectrum by spectrum basis. Both a direct granule to granule estimate and correction and an offline model of the intra-orbital pattern have been implemented to adjust the OMPS NM wavelength scale as part of the N-value computation. The OMPS NP shows little intra-orbit wavelength scale variation but the solar measurements show an annual cycle. This is not currently corrected and represent an error source for the ozone profile products. We plan to implement a correction in 2015.

## 2.4. Algorithm Output

Describe the output data products - not format - at a level of detail to determine if the product meets user requirements. (*Document Object 17*)

**Writers:** Algorithm Scientists.

Table 2-3 describes the external distributed NDEV8P file and Table 2-2 describes the variables in file.

**Table 2-3 NDE Ozone Profile File**

File	Description	Format	Size/file
V8PRO-EDR_v1r0_npp_s201601120127494_e201601120128268_c201603221503000.nc	This is the granule output file containing all the derived variables of the NDEV8P product.	netCDF4	0.2 MB/granule file, ~1100 files/day

**Table 2-4 Ozone Profile Output Granule File Content**

Name	Type	Description	Dimension	Units	Range
Latitude	32 bit Float	Latitude	5 x 5	Degrees	-90 ~ 90
Longitude	32 bit Float	Longitude	5 x 5	Degrees	-180 ~ 180
LatCorner	32 bit Float	Latitude	4 x 5 x 5	Degrees	-90 ~ 90
LonCorner	32 bit Float	Longitude	4 x 5 x 5	Degrees	-180 ~ 180
RelativeAzimuthAngle	32 bit Float	The Relative Azimuth angle	5 x 5	Degrees	-180 ~ 180
SolarAzimuthAngle	32 bit Float	Solar Zenith Angle	5 x 5	Degrees	0 ~ 180
SolarZenithAngle	32 bit Float	Solar Zenith Angle	5 x 5	Degrees	0 ~ 180
ViewingAzimuthAngle	32 bit Float	The satellite azimuth angle	5 x 5	Degrees	0 ~ 180
ViewingZenithAngle	32 bit Float	The viewing zenith angle	5 x 5	Degrees	0 ~ 180
UVAerosolIndex	32 bit	Aerosol Index	5 x 5	Unitless	-100~ 100

	Float				
AlgorithmFlag_TO3	32 bit Integer	Algorithm Flag	5 x 5	Unitless	0 ~ 10
Ascending_Descending	32 bit Integer	1=Descending, 0=Ascending	5 x 5	Unitless	0~ 1
AverageSolutionResidual	32 bit Float	Average of residuals	5 x 5	Nvalue	0~ 20
AveragingKernel	32 bit Float	Averaging kernel matrix at 20 layers	20 x 20 x 5 x 5	DU/DU	-500~ 500
ChannelBandpassFWHM	32 bit Float	The FWHM band width assumption	13	Nanometers	0.2~ 50
CloudPressure	32 bit Float	Cloud Pressure	5 x 5	hPa	10~ 1500
ColumnAmountO3_Profile	32 bit Float	Ozone Profile Column Sum	5 x 5	Dobson Units	0~ 10000
ColumnAmountO3_TO3	32 bit Float	Step 3 ozone	5 x 5	Dobson Units	10~ 1000
CorrelationLength	32 bit Float	The correlation length	1	Unitless	0~ 81
EffectiveCloudFraction	32 bit Float	Radiative Cloudfraction	5 x 5	Unitless	0~ 100
ErrorApriori	32 bit Float	The apriori error covariance matrix assumption	1	Unitless	0~ 10
ErrorCode_Profile	32 bit Integer	Profile Return Code	5 x 5	Unitless	0 ~ 19
ErrorCode_TO3	32 bit Integer	Error flag from the Total ozone computation	5 x 5	Unitless	0 ~ 10
ErrorMeasurement	32 bit Float	The measurement error	10	Unitless	0~ 10
FINALRESIDUAL	32 bit Float	Final Residuals from solution profile	10 x 5 x 5	Unitless	-100~ 100
INITIALRESIDUAL	32 bit Float	Initial Residuals from	10 x 5 x 5	Unitless	-100~ 100

		solution profile			
IndexLongestChannel	32 bit Integer	Index of longest channel used in retrieval	5 x 5	Unitless	1 ~ 500
InformationContent	32 bit Float	Information Content, the trace of the averaging kernel	5 x 5	Unitless	0~ 20
JACOBIAN	32 bit Float	Jacobian from internal forward model	20 x 20 x 5 x 5	Delta_nvalue / Delta_layer_ozone	-1000~ 1000
MidTime	64 bit Float	Elapsed time in seconds since Jan 1, 1958 including leap seconds	15	Microseconds	1.0~ 1.0E12
NValue	32 bit Float	Measure Nvalues at all channels	13 x 5 x 5	Nvalue	10~ 5000
NumberIterations	32 bit Integer	Number of iterations for Convergence	5 x 5	Unitless	1 ~ 100
NvalueAdjustment	32 bit Float	Computed Nvalue soft calibration adjustment	13 x 5	Nvalue	-3~ 3
O3Apriori	32 bit Float	Apriori Ozone Profile	21 x 5 x 5	Dobson Units	0~ 1000
O3BelowCloud	32 bit Float	Ozone below cloud estimate	5 x 5	Dobson Units	0~ 100
O3FINAL	32 bit Float	Ozone Solution Profile	21 x 5 x 5	Dobson Units	0~ 1000
O3Initial	32 bit Float	First Guess Ozone Profile	21 x 5 x 5	Dobson Units	0~ 1000
O3MixingRatio	32 bit Float	ozone volume mixing ratio	15 x 5 x 5	PPMV	0~ 1000
Pressure	32 bit Float	The pressure at the bottom of each layer in the solution profile	21	hPa	0.1~ 1013.25
PressureMixingRatio	32 bit	The pressure	15	hPa	0.5~ 50.0

	Float	levels of the volume mixing ratio profile			
Reflectivity331	32 bit Float	Computed reflectivity at the 331nm channel	5 x 5	Unitless	0~ 100
Reflectivity340	32 bit Float	Computed reflectivity at the 340nm channel	5 x 5	Unitless	0~ 100
Reflectivity380	32 bit Float	Computed reflectivity at the 380nm channel	5 x 5	Unitless	0~ 100
Residual_TO3	32 bit Float	Residuals from total oz calculation	5 x 5 x 5	Dobson Units	-100~ 100
SnowIceFlag	32 bit Integer	Snow Ice flag from Climatology	5 x 5	Unitless	1 ~ 100
StepOneO3	32 bit Float	Step 1 ozone	5 x 5	Dobson Units	10~ 1000
StepTwoO3	32 bit Float	Step 2 ozone	5 x 5	Dobson Units	10~ 1000
SurfaceCategory	32 bit Integer	Scene Type from Lookup Table	5 x 5	Unitless	1 ~ 100
TemperatureClimatology	32 bit Float	Temperature profile used in solution	21 x 5 x 5	Degrees Kelvin	100~ 400
TerrainPressure	32 bit Float	Terrain Pressure from lookup tables	5 x 5	hPa	100~ 1500
WaveLength	32 bit Float	The band centers for all channels	13	Nanometers	260~ 550
Wavelength_Profile	32 bit Float	The band centers for channels used in the profile oz computation	10	Nanometers	260~ 550
Wavelength_TO3	32 bit Float	The band centers for channels used	5	Nanometers	260~ 550

		in the total oz computation			
dndo_TO3	32 bit Float	Ozone sensitivities	5 x 5 x 5	NValue/D obson Unit	-20~ 50
dndr_TO3	32 bit Float	Reflectivity sensitivities	5 x 5 x 5	NValue	0~ 600
quality_information	32 bit Integer	granule quality information attributes	1	percentile	0~ 100
yearday	64 bit Float	The day of year	5 x 5	day	1~ 366

## 2.5. Performance Estimates

### 2.5.1. Test Data Description

The V8Pro algorithms has been used to process the five years (2012-2016) of S-NPP OMPS NP and NM SDRs. Analysis of the results are provided at [https://www.star.nesdis.noaa.gov/smcd/spb/OMPSDemo/proOMPSbeta.O3PRO\\_V8.php](https://www.star.nesdis.noaa.gov/smcd/spb/OMPSDemo/proOMPSbeta.O3PRO_V8.php) and have been use to provide the performance estimates present in the readiness reviews and in this section. These results used the operational SDR products so the quality of the measurements have been improving as the SDR algorithms are updated.

### 2.5.2. Sensor Effects

There are four primary SDR errors related to the ozone product precision and accuracy. They are wavelength scale variations, solar activity variations, instrument degradation and stray light contributions. The sensitivity of the ozone retrievals to radiance::irradiance ratio errors is approximately 1.6%:1%. This sensitivity is used to estimate the impact of the four errors on ozone profile retrievals.

Wavelength scale errors from the uncorrected annual cycle in OMPS NP wavelengths produce radiance variations of  $\pm 1\%$  or greater in radiances leading to 3% ozone profile effects over the full range of variations

$$1.6\%/1\% \times 1\% = 1.6\%$$

There are additional contributions from the ozone cross-section gradient producing 0.4% ozone retrieval effects

$$0.02 \text{ nm} \times 100\%/5 \text{ nm} \times 1\%/1\% = 0.4\%$$

This error will be reduced substantially with the planned use of bi-weekly updates to the OMPS NP SDR wavelength scale and solar spectra.

Solar activity produces irradiance variations of  $\pm 1\%$  or greater at V8Pro channels over a 27-day solar rotation or over the 11-year solar cycle. Since the OMPS NP SDR does not account for these variations, they become  $\pm 1\%$  errors in the radiance to irradiance ratios and produce 3% error in the ozone retrieval over the full range.

$$1.6\%/1\% \times 1\% = 1.6\%$$

This solar activity is modeled in the reprocessing.

The OMPS NP has instrument throughput degradation of approximately 1% over the last five at the shorter channels. If this degradation is corrected annually in the SDR then error will be on the order of 0.3% in ozone.

$$1 \text{ year} \times 1.6\%/1\% \times 0.2\%/year = 0.3\%$$

Stray light errors following the introduction of an SDR correction are now approximately 1/3 of the original errors with scene dependent radiance variations of  $\pm 1\%$ . These primarily contribute to degraded precision of 3%.

$$1.6\%/1\% \times 1\% = 1.6\%$$

### 2.5.3. Retrieval Errors

**Table 2-5 Ozone Profile Performance Requirements**

<b>Ozone Nadir Profile (OMPS-NP) (3)</b>	
<b>Attribute</b>	<b>Threshold</b>
a. Horizontal Cell Size	250 x 250 km <sup>2</sup> (1)
b. Vertical Cell Size	3 km reporting
1. Below 30 hPa ( ~ < 25 km)	10 -20 km
2. 30 -1 hPa ( ~ 25 -50 km)	7 -10 km
3. Above 1 hPa ( ~ > 50 km)	10 -20 km
c. Mapping Uncertainty, 1 Sigma	< 25 km
d. Measurement Range 0-60 km	0.1-15.0 ppmv
e. Measurement Precision (2)	
1. Below 30 hPa ( ~ < 25 km)	Greater of 20 % or 0.1 ppmv

2. 30 -1 hPa ( ~ 25 -50 km)	5% -10%	
3. Above 1 hPa ( ~ > 50 km)	Greater of 10% or 0.1 ppmv	
f. Measurement Accuracy (2)		
1. Below 30 hPa ( ~ < 25 km)	Greater of 10 % or 0.1 ppmv	
2. 30 -1 hPa ( ~ 25 -50 km)	5% -10%	
3. Above 1 hPa ( ~ > 50 km)	Greater of 10 % or 0.1 ppmv	
g. Refresh	At least 60% coverage of the globe every 7 days (monthly average) (2,3)	
<p><b>Notes:</b> 1. SDRs will go to 50x50 km<sup>2</sup> for J-01. 2. The OMPS Nadir Profiler performance is expected to degrade in the area of the South Atlantic Anomaly (SAA) due to the impact of periodic charged particle effects in this region. 3. All OMPS measurements require sunlight, so there is no coverage in polar night areas.</p>		

Verification of Performance:

- a. 93-Pixel cross-track aggregation and 37.5-S along track integration.
- b. Version 8 Algorithms Averaging Kernels
- c. Confirmed by to Nadir Mapper, Pixel size, and co-alignment.
- d. Confirmed by five years of processing and ground-based matchup scatter.
- e. Precision estimates from SNR and Version 8 measurement contribution functions, and along-track differences
- f. Accuracy is adjusted by soft calibration and checked by zonal mean statistics, chasing orbits, and Version 8 a priori profiles
- g. Suborbital track and precession of orbits.

### 2.5.4. Numerical Computation Considerations

The algorithm is an inverse problem using a maximum likelihood approach. The A Priori profiles are provide from a climatological database described above. Initial estimates of the total ozone are used to generate a first guess to start the iterative linearization process for the optimal estimation retrieval. The forward model combines fast and accurate single scattering radiance estimates with adjustments from table values of multiple scattering components and their Jacobians. The algorithm works with 12 measurements and 81 layers so the matrix inverse problems are not particularly computation intensive. Double

precision computations maintain sufficient accuracy. In addition, the relatively large FOVs mean that a day's worth of data can be processed in minutes.

### **2.5.5. Programming and Procedural Considerations**

The algorithm requires both OMPS NP and OMPS NM SDR and GEO files. The OMPS NM measurements are made with small FOVs so the collocated measurements have to be identified and averaged to match the OMPS NP FOV. The OMPS NM measurements may be spread across two granules.

### **2.5.6. Quality Assessment and Diagnostics**

The product quality is monitored at

[https://www.star.nesdis.noaa.gov/smcd/spb/OMPSSDemo/proOMPSbeta.O3PRO\\_V8.php](https://www.star.nesdis.noaa.gov/smcd/spb/OMPSSDemo/proOMPSbeta.O3PRO_V8.php)  
for the EDR products and at

[https://www.star.nesdis.noaa.gov/icvs/status\\_NPP\\_OMPS\\_NP.php](https://www.star.nesdis.noaa.gov/icvs/status_NPP_OMPS_NP.php)

and

[https://www.star.nesdis.noaa.gov/icvs/status\\_NPP\\_OMPS\\_NM.php](https://www.star.nesdis.noaa.gov/icvs/status_NPP_OMPS_NM.php)

The products progress through the standard validation from beta, to provisional, to validated stages 1, 2 and 3.

### **2.5.7. Exception Handling**

The algorithm checks for non-physical values for radiances and irradiances and terminates the retrieval if invalid quantities are detected. The product file for these cases contain fill values for the ozone retrievals. Additional error and algorithm flags are identified in the SMM and EUG.

## **2.6. Validation**

The V8Pro algorithm has been used as the operational algorithm for the NOAA POES SBUV/2 instruments since 2000.

## **3. ASSUMPTIONS AND LIMITATIONS**

### **3.1. Performance Assumptions**

While the algorithm performance requirements are for SZA less than 80°, it provide good results even for higher SZAs and in regular operations it is applied for SZA out to 86°. The algorithm also flags eclipse conditions that lead to poor performance, as the solar signal reduction is complex. There is another performance exclusion for measurements made in the South Atlantic Anomaly (SAA) as the OMPS NP measurements are significantly affected by the charged particles in this region.

## **3.2. Potential Improvements**

The algorithm can make use of more channels than the current 10 used for ozone profile retrievals. The main benefit of the additional channels is a reduction in the effects of measurement noise. This can also be obtained by using information concentration methods such as principal component analysis or simple polynomial regression over wavelength intervals about given channels.

---

#### 4. REFERENCES

List all references to external documents.

- Ball Aerospace & Technology Corporation, Algorithm Theoretical Basis Document (ATBD) Nadir Profile Ozone) for the Ozone Mapping and Profiler Suite (OMPS) of the National Polar-Orbiting Operational Environmental Satellite System (NPOESS) Program, Document Number – IN0092A-108 CI Number – SS0052Am January 2002.
- Bates, D.R., “Rayleigh scattering by air,” *Planet. Sp. Sci.*, **32**, 785-790, 1984.
- Bhartia, P.K., *et al.*, “Applications of the Langley plot method to the calibration of SBUV instrument on Nimbus-7 satellite,” *J. Geophys. Res.*, **100**, 2997-3004, 1995.
- Bhartia, P.K., *et al.*, “Algorithm for the estimation of vertical profiles from the backscattered ultraviolet technique,” *J. Geophys. Res.* **101**, 18,793-18,806, 1996.
- Cebula, R.P., & DeLand, M.T., “Comparisons of the NOAA-11 SBUV/2, UARS SOLSTICE, and UARS SUSIM Mg II solar activity proxy indexes,” *Solar Physics*, **177**, 117–132, 1998.
- Chapman, S., “The absorption and dissociative or ionizing effect of monochromatic radiation in an atmosphere on a rotating earth,” *Proc. Phy. Soc. (London)*, **43**, 483-501, 1931.
- Deland, M.T., *et al.*, NOAA-17 SBUV/2 (Flight Model#6) Activation and Evaluation Phase (A&E) Report, SSAI Document #SSAI-2015-180-MD-2002-02, 2002.
- Michael G. Dittman ; Eric Ramberg ; Michael Chrisp ; Juan V. Rodriguez ; Angela L. Sparks ; Neal H. Zaun ; Paul Hendershot ; Tom Dixon ; Robert H. Philbrick and Debra Wasinger "Nadir ultraviolet imaging spectrometer for the NPOESS Ozone Mapping and Profiler Suite (OMPS)", Proc. SPIE 4814, Earth Observing Systems VII, 111 (September 25, 2002); doi:10.1117/12.453748; <http://dx.doi.org/10.1117/12.453748>.
- Fleig, A.J., *et al.*, Nimbus 7 Solar Backscatter Ultraviolet (SBUV) Ozone Products User's Guide, NASA Reference Publication 1234, 1990.
- Flynn, L.E., *et al.*, 2000, “Internal validation of SBUV/2 ozone vertical profile data sets,” Proceedings of the Quadrennial Ozone Symposium, Sapporo, 75-76.
- Flynn, L.E. *et al.*, “Characterization of Operational Solar Backscatter Ultraviolet Instruments at the U.S. NOAA,” Proceedings of ACVE-3, ESA, Frascati Italy, December 4-7, 2006.
- Frederick, J.E, R.P. Cebula, & D.F. Heath, “Instrument characterization for the detection of long-term changes in stratospheric ozone: An analysis of the SBUV/2 radiometer,” *J. Atmos. Oceanic Technol.*, **3**, 472-480, 1986.
- Gleason, J.F, & R.D. McPeters, “Correction to the Nimbus 7 solar backscatter ultraviolet data in the "nonsync" period (Feb. 1987 to June 1990),” *J. Geophys. Res.*, **100**, 16,873-16,877, 1995.
- Heath, D.F., *et al.*, “The solar backscatter ultraviolet and total ozone mapping spectrometer (SBUV/TOMS) for Nimbus G,” *Optical Engineering*, **14**, 323-331, 1975.
- Heath, D.F., *et al.*, "Comparison of Spectral Radiance Calibrations of SSBUV-2 Satellite Ozone Monitoring Instruments using Integrating Sphere and Flat-Plate Diffuser Technique," *Metrologia*, **30**, 259-264, 1993.

- 
- Herman, J.R., *et al.*, “A new self-calibration method applied to TOMS and SBUV backscattered ultraviolet data to determine long-term global ozone change,” *J. Geophys. Res.*, **96**, 7531-7545, 1991.
- Hilsenrath, E., *et al.*, “Calibration of the NOAA-11 Solar Backscatter Ultraviolet (SBUV/2) Ozone Data Set from 1989 to 1993 using In-Flight Calibration Data and SSBUV,” *J. Geophys. Res.*, **100**, 1351-1366, 1995.
- Huang, L.K., *et al.*, “Determination of NOAA-11 SBUV/2 radiance sensitivity drift based on measurements of polar ice cap radiance,” *Int. J. Remote Sensing*, **24**(2),305-314, 2003.
- Meijer, Y., *et al.*, “Evaluation of global ozone monitoring experiment (GOME) ozone profiles from nine different algorithms, *J. Geophys. Res.*, **111**, D21306, doi: 10.1029/2005JD006778, 2006.
- Rodgers, C.D., “Retrieval of atmospheric temperature and composition from remote measurements of thermal radiation,” *Rev. Geophys. Space Phys.*, **14**, 609-624, 1976.
- Rodgers, C.D., The Characterization and Error Analysis of Profiles Retrieved from Remote Sounding Measurements, *J. Geophys. Res.*, **95**, 5587-5595, 1990.

#### Web References

The Solar Backscatter Ultraviolet instrument (SBUV/2) measurements fly on the NOAA Polar-orbiting Operation Environmental Satellites (POES). Information on these sensors and products is available in sections 3.8, 7.4 and 9.7 of the NOAA-KLM User’s Guide at <http://www.ncdc.noaa.gov/docs/klm/>.

Activation and evaluation reports and other calibration documents can be found at <http://www.orbit.nesdis.noaa.gov/smcd/spb/calibration/icvs/sbuvd/doc.html>

Calibration and validation monitoring can be found in the ultraviolet instrument links at <http://www.orbit2.nesdis.noaa.gov/smcd/spb/calibration/icvs/index.html>

Additional monitoring information and the V8 Fortran code are available from links at <http://www.orbit.nesdis.noaa.gov/smcd/spb/ozone/>  
<ftp://www.orbit.nesdis.noaa.gov/pub/smcd/spb/ozone/code>

Additional documentation and product validation are contained on the V8PRO data DVD available at

<http://disc.sci.gsfc.nasa.gov/data/datapool/TOMS/DVD-ROMs/>

The following documents with information on the V8TOZ and V8PRO implementation in the operational processing at NOAA are available from NOAA/NESDIS:

Solar Backscattered Ultraviolet Radiometer (SBUV/2) Operational Ozone Product System Version 8, **System Maintenance Manual**, Dec. 2006, Prepared by Q. Zhao & J. Selekof.

Solar Backscattered Ultraviolet Radiometer (SBUV/2) Operational Ozone Product System Version 8, **System Description Document**, Dec. 2006, Prepared by Q. Zhao & J. Selekof.

Solar Backscattered Ultraviolet Radiometer (SBUV/2) Operational Ozone Product System Version 8, **Interface Control Document**, Dec. 2006, Prepared by Q. Zhao & J.

Selekof, Z., Ahmad, & P.K. Bhartia, "Effect of Molecular Anisotropy on the Backscattered UV Radiance," *Appl. Opt.*, **34**, 8309-8314, 1995.

---

END OF DOCUMENT